Diagnosing a Colorado Heavy Snow Event with a Nonhydrostatic Mesoscale Numerical Model Structured for Operational Use

JOHN S. SNOOK

Forecast Systems Laboratory, National Oceanic and Atmospheric Administration, Boulder, Colorado

ROGER A. PIELKE

Department of Atmospheric Science, Colorado State University, Fort Collins, Colorado

(Manuscript received 28 June 1994, in final form 1 December 1994)

ABSTRACT

State-of-the-art data sources, such as Doppler radar, automated surface observations, wind profiler, digital satellite, and aircraft reports, are for the first time providing the capability to generate real-time, operational three-dimensional gridded datasets with sufficient spatial and temporal resolutions to diagnose the structure and evolution of mesoscale systems. A prototype data assimilation system of this type, called the Local Analysis and Prediction System (LAPS), is being developed at the National Oceanic and Atmospheric Administration's Forecast Systems Laboratory. The investigation uses the three-dimensional LAPS analyses for initialization of the nonhydrostatic Regional Atmospheric Modeling System (RAMS) model developed at Colorado State University to create a system capable of generating operational mesoscale predictions. The LAPS/RAMS system structured for operational use can add significant value to existing operational model output and provide an improved scientific understanding of mesoscale weather events. The results are presented through a case study analysis, the 7 January 1992 northeast Colorado blizzard. The case is ideal for this investigation because of the significant mesoscale variation observed in the precipitation and flow structure. The case study results demonstrate the ability to successfully detect and predict mesoscale features using a mesoscale numerical model initialized with high-resolution (10-km horizontal grid interval), nonhomogeneous data. A conceptual model of the snowstorm is developed by using the RAMS model output in combination with observations and other larger domain model simulations. The LAPS/RAMS system demonstrates the ability to operationally forecast and display mesoscale systems in the local weather office.

1. Introduction

State-of-the-art data sources, such as Doppler radar, automated surface observations, wind profiler, digital satellite, and aircraft reports, are providing a vastly improved view of the atmosphere to the operational meteorological community. Using these data sources, three-dimensional gridded datasets can be assembled in real time with sufficient spatial and temporal resolutions to diagnose the structure and evolution of mesoscale systems.

A data assimilation system of this type, called the Local Analysis and Prediction System (LAPS) (McGinley 1989; McGinley et al. 1991), is being developed at the National Oceanic and Atmospheric Administration's Forecast Systems Laboratory (FSL). LAPS integrates all available data to generate real-time, high-resolution (10-km horizontal grid interval), three-dimensional analyses of meteorological state variables and is designed to perform operationally in a local weather forecast office (McGinley 1995).

Three-dimensional LAPS analyses afford the opportunity to initialize a full-physics, nonhydrostatic mesoscale numerical model with operational (nonhomogeneous) data at resolutions (~10-km horizontal grid interval) finer than previously feasible. This investigation is unique because it is one of the first attempts to initialize a high-resolution numerical forecast model with comparable high-resolution operational analyses. Also, advances in desktop computer workstation and data storage technology are providing the capability to produce mesoscale numerical forecasts in real time at a reasonable cost (Cotton et al. 1994). Three-dimensional visualization techniques, available with the advanced desktop computer workstations, enable the forecaster to display and interpret the enormous amounts of data generated by the mesoscale forecast model in a reasonable amount of time. Results from this study demonstrate, for the first time, a real-time analysis and prediction system capable of forecasting and displaying mesoscale systems in the local weather office.

Corresponding author address: Dr. John S. Snook, Forecast Systems Laboratory, National Oceanic and Atmospheric Administration, Boulder, CO 80303.

The objectives of this paper are 1) to evaluate the accuracy of forecasts from a mesoscale numerical model initialized with high-resolution, nonhomogeneous data; 2) to determine if the model forecasts can detect mesoscale features, hence adding value to currently available regional-scale model forecasts; and 3) to demonstrate the ability to use the model output to provide an improved scientific understanding of mesoscale weather events. Wesley (1991) notes that the Colorado Front Range is an excellent laboratory for winter storm studies due to the wide variety of meteorological phenomena. Since these phenomena often exhibit significant mesoscale variation, the Colorado Front Range is an ideal location to evaluate mesoscale model forecasts. The objectives will be addressed by initializing the Regional Atmospheric Modeling System (RAMS) developed at Colorado State University with LAPS analyses from a significant Colorado Front Range snowstorm that occurred on 7 January 1992. Strong winds, heavy snowfall, and significant mesoscale precipitation variation were observed in this case.

A review of previous research related to this investigation is discussed in section 2. The experiment design is presented in section 3. The case study diagnosis and RAMS simulations are described in section 4, followed by a discussion and conclusions.

2. Colorado Front Range winter storms

A recent overview of dynamically forced heavy snowfall investigations is discussed by Marwitz and Toth (1993). A unique aspect of diagnosing Colorado Front Range winter storms is that in addition to considering dynamical forcing, the influence of the complex Colorado terrain must also be incorporated. Since a wide variety of terrain-influenced weather phenomena affects the Colorado Front Range, numerous field projects and case study analyses have been conducted over this region. Observational analyses of significant weather events have provided pertinent conceptual models. More recently, numerical simulations of Front Range winter storms have provided further insight into the processes important to describing meteorological phenomena over mountainous terrain. An overview of the literature pertinent to this investigation is presented in the following sections.

a. Observational studies

Significant winter precipitation along the Colorado Front Range is typically associated with synoptically driven easterly "upslope" flow, opposite in direction from the climatologically prevailing westerlies (Reinking and Boatman 1986). These upslope events are normally categorized into two types: 1) systems with fully developed, deep cyclonic circulations; and 2) shallow anticyclonic systems. Wesley (1991) also cites cases where both circulations are important at different atmospheric levels. Most observational studies of Colorado Front Range winter storms have concentrated on the effects of the upslope circulations interacting with the complex terrain. For some winter storm cases, the juxtaposition of prevailing westerlies and easterly upslope circulations further complicates an already intricate situation. These cases present difficult forecast problems with sharp gradients in precipitation typically observed. Recognizing the implications of the various flow interactions and how to better forecast them are important aspects of this investigation.

The typical heavy snow-producing Colorado Front Range winter storm has been described with a storm composite structure (Fawcett and Saylor 1965; Howard and Tollerud 1988; Tollerud et al. 1991). The results describe a typical scenario of a fully developed, deep cyclonic event. The composite storm evolution shows the cyclone to emanate from an eastern Pacific developmental trough and begin to deepen over the northwest portion of the United States. The storm track for the middle and late cyclone stages moves southeastward across the Four Corners region and then northeastward into the Midwest.

Reinking and Boatman (1986) provide a comprehensive description of upslope precipitation events. Numerous observational case studies have discussed the tremendous mesoscale variability that often occurs in the observed snowfall with Front Range winter storms. For instance, Schlatter et al. (1983) noted a snowfall gradient of 1.0 m across a distance of only 90 km associated with a December 1982 deep cyclonic storm. The use of high-resolution instrumentation—such as Doppler radar, automated surface observations, and wind profilers—has enabled a more complete diagnosis of the spatial snowfall variations (e.g., Lilly 1981; Schlatter et al. 1983). However, Schlatter et al. noted that the variations are difficult to explain quantitatively and there is much to learn before the details of these storms can be forecasted accurately.

The development of embedded heavy snow bands typically contributes to the extreme variability in observed snowfall. The bands have been associated with a variety of phenomena, including topographical forcing (e.g., Reinking and Boatman 1986), cold-air damming (e.g., Dunn 1987; Wesley and Pielke 1990), low-level barrier jets (e.g., Dunn 1992), conditional symmetric instability (e.g., Snook 1992), and dynamical forcing (e.g., Dunn 1988).

b. Numerical simulations of Front Range winter storms

Only a few numerical simulations of Colorado Front Range winter storms appear in the literature. Operational models with spatial resolutions too coarse to resolve the mesoscale details often provide inadequate predictions of Front Range snowstorms (e.g., Papineau 1992). Advances in mesoscale modeling during the

past decade (e.g., Ross 1986) have presented the opportunity to investigate and forecast Front Range winter storms in greater detail. Increased model grid resolution allows an improved representation of the complex orography. Hence, the investigations published thus far have primarily concentrated on the effects of topography on Front Range weather.

Several model simulations using RAMS with horizontally uniform initialization were performed by Abbs and Pielke (1987) and Wesley et al. (1990) to investigate orographic effects on northeast Colorado snowstorms. These simulations demonstrated that the model could successfully predict the relationship between the prevailing wind direction and observed snowfall distribution, which correlated closely with terrain forcing.

The first attempt to simulate a Front Range winter storm using a mesoscale model initialized with nonhomogeneous data was accomplished by Wesley (1991). RAMS was initialized with National Meteorological Center (NMC) objective analyses for the deep cyclonic storm of 30–31 March 1988. The inner grid horizontal increment was 22 km and a full microphysics version of the model was employed. The simulation successfully depicted the development of strong upslope flow and heavy precipitation. When compared to operational model forecasts from NMC, the RAMS forecast of orographic enhancement of precipitation was much more accurate. Increased spatial grid resolution and improved topographical representation were significant contributors to this improvement. The results also indicate the importance of quality model initialization and further experimentation with improved model initialization was suggested. Recent additions to the observational network along the Front Range, including Doppler radar, wind profiler, automated surface observations, and digital satellite data, are enabling improved atmospheric analyses, offering the opportunity to investigate Front Range winter storms in much greater detail than previously possible.

c. Numerical simulations using operational data

Historically, as data resolution and quality improve, as model numerics become more sophisticated, as communication capabilities increase, and as computers become faster, operational numerical model prediction uses smaller grid resolutions. Numerical modeling using operational data has been progressing toward higher spatial resolutions and is just now entering the mesoscale resolutions necessary to have any chance of forecasting the mesoscale variation often observed in Front Range winter storms. Ross (1986) provides a brief history of operational numerical weather prediction in the United States. Despite steady improvement in operational numerical forecasts, the operational models still have problems with wintertime systems containing low-level arctic air masses over the High Plains (Junker et al. 1989; Wesley 1991) and orographically influenced features (Rasmussen et al. 1992). Increased resolution of observations and improved model grid resolutions are necessary to provide better forecasts of winter storms in the vicinity of mountains. Research applications using mesoscale models with improved initialization are beginning to achieve this goal.

Warner and Seaman (1990) describe a real-time experimental mesoscale modeling system at The Pennsylvania State University (PSU). A hydrostatic version of the PSU/National Center for Atmospheric Research (NCAR) Mesoscale Model with a 30-km inner grid increment is used to generate numerical weather forecasts for the northeastern United States. Operational data obtained from NMC are automatically combined with local observations to provide analyses for model initialization. Real-time model output for two case studies demonstrates the capability to provide greater detail in forecast fields of pressure, wind, and precipitation when compared to the NMC operational model output. In addition to improved forecasts, the real-time system has led to enhanced conceptual models and improvements in model physics. A similar configuration of the PSU/NCAR Mesoscale Model, Version 4 (MM4) was implemented during the Winter Icing and Storms Project 1991 (WISP91) to aid in operational planning (Rasmussen et al. 1992). A hydrostatic version of the PSU/NCAR Mesoscale Model, Version 5 (MM5) with warm water microphysics and a 20-km inner grid was implemented to support the Storm scale Operational and Research Meteorology-Fronts Experiment and Systems Test (STORM-FEST) during the winter of 1992. A nonhydrostatic version of MM5 has been recently developed and successfully tested on idealized and real-data simulations (Dudhia 1993).

FSL is tasked with demonstrating the feasibility of operating real-time analysis and prediction systems at even smaller grid resolutions. The Mesoscale Analysis and Prediction System (MAPS) was developed on a 60-km national scale grid using 25 sigma/isentropic hybrid levels (Benjamin et al. 1991) to provide updated model analyses and forecasts every 3 h. MAPS has been implemented at NMC as the Rapid Update Cycle (RUC). The first attempts to use MAPS as an initialization to a full physics, nonhydrostatic numerical model (i.e., RAMS) is discussed by Schmidt and Snook (1992) and Thompson (1993). Thompson provided daily real-time forecasts using RAMS with a 25-km inner grid and initialized with MAPS for the winters of 1991–92 and 1992–93. Results indicated improvements over current operational models in forecasts of temperature, geopotential height, and wind. Improvements in precipitation amounts were obtained only when using a full microphysics version of the model.

The FSL 10-km grid increment LAPS generates regional scale analyses of atmospheric variables every hour. Snook and Schmidt (1992) describe the initial attempt to use LAPS as an initialization to RAMS. Since LAPS incorporates mesoscale data not available

to national scale analyses, a LAPS model initialization should improve mesoscale model forecasts. This investigation uses LAPS analyses as RAMS initialization to investigate the possibilities of generating real-time mesoscale predictions. Model output will be compared to other operational forecasts to verify if real-time mesoscale models can enhance the local short-range (0–12-h) prediction.

3. Experiment design

A unique aspect of this investigation is to initialize a mesoscale numerical model (RAMS) with comparable resolution LAPS operational analyses that have incorporated all conventional and state-of-the-art data sources. Furthermore, the system is designed to function operationally in the local weather forecast office on affordable computer workstations (Snook et al. 1995). RAMS is a full physics, nonhydrostatic primitive equation model developed as a merger of several previous models (Wesley 1991; Pielke et al. 1992). The complexity of the model physics is controllable through a menu-driven selection list. A discussion of the operational data sources, the model configuration and initialization procedures for the case study simulation, and the model validation methods follows.

a. The Mesoscale Analysis and Prediction System—MAPS

MAPS provides the capability to investigate mesoscale phenomena in greater detail than previously possible with operational NMC analysis products. The inclusion of numerous aircraft reports and wind profiler data, in addition to other conventional observations, allows MAPS to generate upper-air analyses of the atmospheric state variables every 3 h on a national 60-km grid increment domain (Benjamin et al. 1991; Smith and Benjamin 1993). The system uses a 25 sigma/isentropic level hybrid coordinate system that provides increased resolution in the vicinity of highly baroclinic features. MAPS generates 12-h forecasts every 3 h using a hydrostatic numerical scheme with the primary intent of providing background fields for future analyses. MAPS is run operationally at FSL and routinely interpolates the analyses and forecasts to a standard isobaric coordinate system for display on the prototype National Weather Service meteorological computer workstation.

b. The Local Analysis and Prediction System—LAPS

LAPS provides even greater mesoscale detail on a local Colorado forecast domain by enhancing the MAPS analyses with the addition of available local data sources. Local datasets include 5-min surface observations from FSL's 22 station automated mesonet, the prototype WSR-88D Doppler radar located about 10 km northeast of Denver, the wind profiler data located at Platteville, Colorado, and digital infrared satellite data ingested at FSL directly from the Geostationary Operational Environmental Satellite (GOES, Fig. 1). LAPS uses a regional 10-km grid increment domain covering most of Colorado and small portions of adjacent states (Fig. 2) to provide surface and three-dimensional analyses of atmospheric state variables every hour (McGinley 1989; McGinley et al. 1991). The LAPS grid is nested exactly within the national 60-km grid interval MAPS domain. The LAPS domain covers a 600 × 600 km area in the horizontal and uses 21 isobaric levels from 1100 to 100 mb with a constant 50-mb increment. LAPS terrain (Fig. 2) is derived from the Defense Mapping Agency (DMA) 30-s spatial interval elevation data by averaging all DMA elevations within each LAPS 100 km^2 grid box area.

The LAPS three-dimensional univariate wind analyses incorporate Doppler radar, wind profiler, aircraft reports, automated surface observations, MAPS, and other conventional data sources (Albers 1989). Height and temperature information are obtained solely from the 60-km MAPS analyses and forecasts. The LAPS moisture analyses use digital satellite and microwave radiometer data to add mesoscale detail to the MAPS moisture fields (Birkenheuer 1991). LAPS also generates separate surface analyses of atmospheric state variables (McGinley et al. 1991) in addition to the three-dimensional analyses. Digital satellite data and

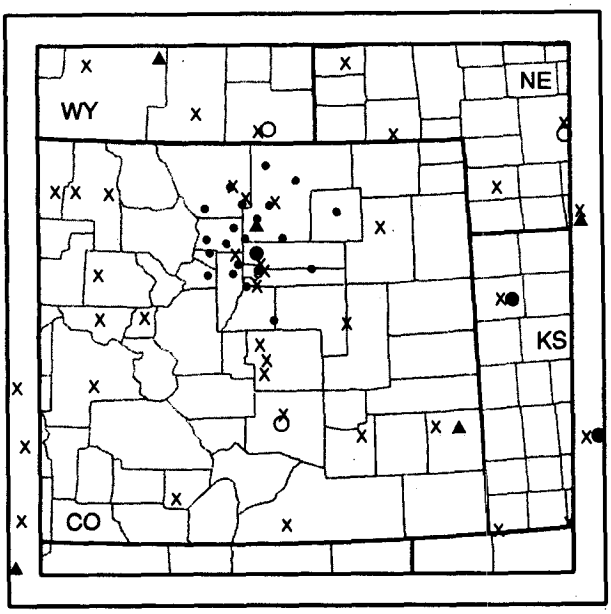

FIG. 1. Weather data available in northeast Colorado. Derived from McGinley et al. (1991).

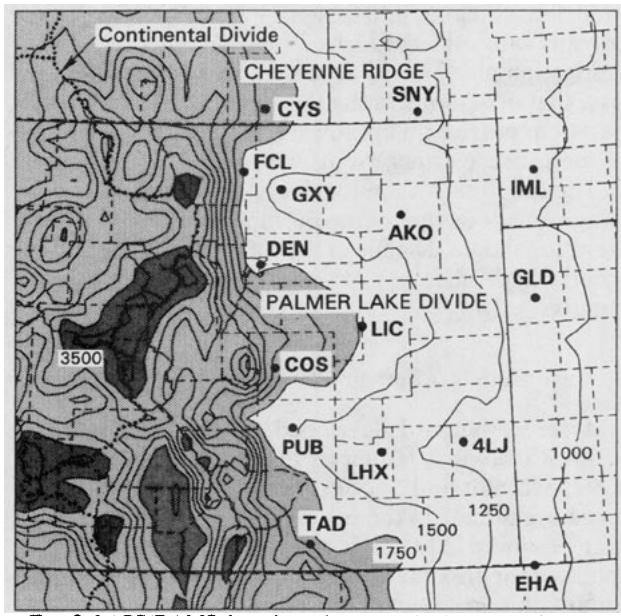

FIG. 2. LAPS/RAMS domain and topography (m). Elevation contour interval is 250 m. Light shaded area indicates terrain above 1750 m, and dark shaded regions indicate terrain above 3500 m. Solid lines depict state boundaries and dashed lines indicate county boundaries. The Continental Divide is denoted by the dotted line. Surface Aviation Observations (SAO) locations east of the Continental Divide are indicated by standard three-letter abbreviations (CYS = Cheyenne, SNY = Sidney, FCL = Fort Collins, GXY = Greeley, AKO = Akron, IML = Imperial, DEN = Denver, GLD = Goodland, LIC = Limon, COS = Colorado Springs, PUB = Pueblo, LHX = LaJunta, 4LJ = Lamar, TAD = Trinidad, EHA = Elkhart).

automated surface observations provide mesoscale detail to the other available surface data sources.

c. *Model initialization and grid configuration*

RAMS is initialized with operational nonhomogeneous data from LAPS and MAPS for the case study to evaluate the accuracy of mesoscale numerical forecasts and demonstrate the ability to use the model output to provide an improved scientific understanding of mesoscale weather events. The RAMS mesoscale numerical model is configured such that the LAPS analyses can be used as model initialization with as little manipulation to the initial fields as possible. Table 1 summarizes the model configuration for the case study simulations. The horizontal model domain is equivalent to LAPS (i.e., 61 × 61 grid points with a 10-km grid increment). The vertical grid is a stretched sigma-z coordinate system with a 300-m grid spacing nearest the ground, a stretch factor of 1.1, and a maximum grid spacing of 750 m. Hence, the model top is approximately 15.3 km above the surface. The vertical grid spacing is designed to maintain all the available resolution in the LAPS analyses while foregoing any greater resolution to allow implementation in real time. Model topography is set equal to the LAPS terrain and is not smoothed to facilitate the inclusion of LAPS surface data without interpolation.

A time-dependent lateral boundary condition is implemented that uses a Davies (1976) nudging scheme to force the model variables toward analyzed values derived from MAPS real-time forecasts. The 600 km × 600 km domain may be small for the type of mesoscale forecasts that will be attempted. Adverse effects from the lateral boundaries may contaminate the results especially after several hours of prediction. For instance, a parcel traveling at 20 m s^{-1} would traverse the entire domain in less than 9 h. The domain was selected to match the available operational data analyses (i.e., LAPS). If the proposed model grid is insufficient in size, a larger, possibly nested, grid system may be required. The downside to a larger grid system is that it may not be feasible to run in real time given the current computer capabilities at FSL.

The LAPS isobaric analyses are linearly interpolated in the vertical to the RAMS sigma-z coordinate system. Horizontal interpolation is not required because the model points correspond exactly with the LAPS analysis points. The separate LAPS surface analyses are blended into the three-dimensional analyses up to 500 m AGL using a height-weighted average of the two analyses such that the surface data receives full weight at the model ground level, whereas the three-dimensional analysis receives full weight at 500 m AGL.

Experiments are conducted using two model configuration variations (with abbreviations for future reference): 1) 10-km three-dimensional LAPS analyses with LAPS surface data blended in (LSFC); and 2) 10-km three-dimensional LAPS analyses with blended LAPS surface data and an explicit representation of microphysics employed (LMIC). The effects of microphysics and precipitation will be evaluated through the LMIC simulations.

d. *Model physics*

RAMS model physics are selected to complement the grid-scale resolution and the winter season meteorology. The model physics are summarized in Table 2. A nonhydrostatic version of the model is employed with two levels of moisture complexity. First, condensation of water vapor to cloud water occurs wherever supersaturation is attained. However, other forms of liquid or ice water are not considered. The second level

TABLE 1. Model grid configuration for case study simulations.

Model category	Option
Grid dimensions	61 × 61 × 25
Horizontal grid increment	10 km
Vertical grid increment	300 m stretched to 750 m
Model top height	15.3 km
Topography	LAPS

TABLE 2. Model physics for case study simulations.

Model category	Option
Initialization	LAPS real-time analyses
Thermodynamics	nonhydrostatic 1) water vapor and cloud water 2) full microphysics
Radiation	radiative effects of water vapor and clouds
Cumulus parameterization	none
Lateral boundary condition	Davies relaxation to MAPS forecasts
Top boundary condition	rigid lid with modified Rayleigh friction-absorbing layer
Surface boundary condition	0.5 m, 11-level soil model
Turbulence	deformation K closure
Time step	30 s

of moisture complexity is to implement microphysical parameterizations of liquid and ice. Five microphysical species, rainwater, pristine ice, snow, aggregates, and graupel, are included (Flatau et al. 1989). A radiation parameterization scheme that includes the radiative effects of liquid and ice water (Chen and Cotton 1983) is used. The cumulus parameterization options in RAMS are not employed. A rigid lid with a modified Rayleigh friction-absorbing layer (Cram 1990) five grid points deep is used for the top boundary condition. At the surface, a 0.5-m, 11-level soil model (Tremback and Kessler 1985) is used. Soil temperatures at all levels are initially set equal to the analyzed surface temperature. Soil moisture initialization is based on the analyzed surface relative humidity. Turbulence closure is accomplished using a deformation K scheme (Smagorinsky 1963; Tremback 1990).

e. Model validation

Model validation is necessary to address two objectives of this investigation: 1) evaluating the accuracy of a mesoscale numerical model initialized with operational nonhomogeneous data, and 2) comparing the forecast accuracy with the performance of other operational model predictions. One of the more difficult tasks in mesoscale numerical model research is quantifying the accuracy of the model predictions. The difficulties are primarily due to the lack of observational data on the scale of this investigation (Thompson 1993). Model validation will be attempted through both qualitative and quantitative approaches.

The qualitative evaluation applies the meteorologists' analysis skills and experience with mesoscale weather phenomena to subjectively compare model predictions with the physical observations and other visual accounts (e.g., human observations, media reports) of the case study. Although not as robust as a quantitative approach, the qualitative evaluation can ascertain the existence of particular features within the model predictions and is useful for subjective comparison with other model output. The qualitative investigation also aids in accomplishing another objective, that of demonstrating the ability to use the model output to provide an improved scientific understanding of mesoscale weather events.

The quantitative approach applies statistical verification methods that compare model output with observational data. Details of the quantitative validation scheme and validation results are presented in the appendix.

4. Case study—7 January 1992

A severe blizzard developed east of the Colorado Front Range on 7 January 1992 (Snook and Schmidt 1992; Schmidt and Snook 1992). The storm is of interest because of 1) the sustained band of heavy snow that produced 20–40 cm of snowfall along a north–south line approximately 40 km east of the Front Range mountain barrier, while the barrier itself received less than 5 cm of snowfall; and 2) the strong gusty surface winds in excess of 20 m s^{-1} that generated blizzard conditions across eastern Colorado for most of the day. Denver received a new 24-h record January snowfall of 34.8 cm and a storm total of 37.6 cm (Fig. 3). The band of heaviest observed snowfall was coincident with Colorado's primary north–south thoroughfare (I-25) and caused major transportation problems that stranded hundreds of motorists (NOAA 1992). The combination of strong surface winds and heavy snow forced numerous road closures and Stapleton International Airport ceased operations for several hours.

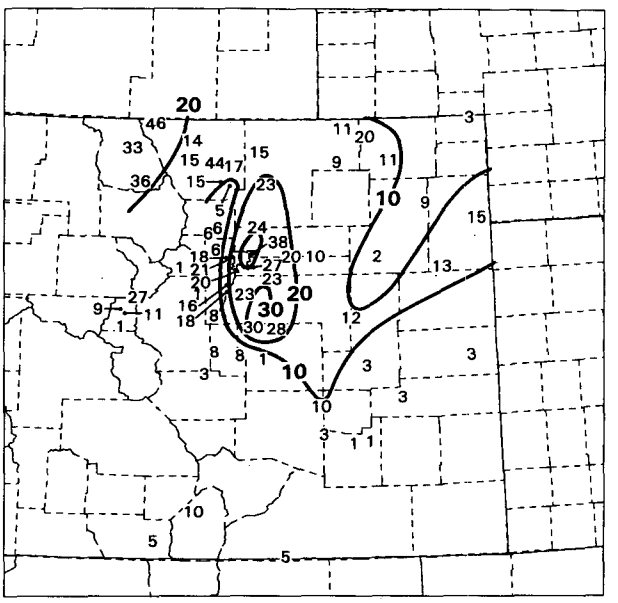

FIG. 3. Observed snowfall (cm) during the 7 January 1992 snowstorm.

The considerable spatial variability within the observed wind and snowfall distributions makes this storm an excellent case to address the mesoscale numerical forecast objectives of this investigation.

a. Synoptic-mesoscale overview

The 7 January 1992 storm exhibited many characteristics of a typical Colorado Rocky Mountain heavy snow event with one significant exception, the development of strong surface westerly winds east of the Continental Divide. The development of the westerlies and their impact on the observed snowfall and other surface characteristics is traced in a presentation of the storm overview.

1) SYNOPTIC-SCALE OBSERVATIONS

NMC analyses of the 500-mb height and isotachs (Fig. 4) show a significant open short wave located over the western United States at 1200 UTC 6 January 1992. A 35 m s^{-1} jet maximum is analyzed curling around the base of the trough. The 500-mb wave traveled eastward across Utah and closed off with a central height of 5406 m over southcentral Colorado by 1200 UTC 7 January. The 35 m s^{-1} jet streak continued to occupy the base of the trough at 0000 UTC 7 January and moved through the trough axis by 1200 UTC 7 January. The evolution of the 500-mb height field closely resembles the composite analyses of a typical Colorado heavy snowstorm (Fawcett and Saylor 1965). The system is clearly categorized as a deep cyclonic circulation type as defined by Reinking and Boatman (1986). The period of moderate to heavy snow at Denver occurred primarily between 1400 and 2000 UTC 7 January, during which time the 500-mb low deepened to 5372 m and progressed slowly northeastward to the western Kansas–Nebraska border. The jet streak strengthened to greater than 40 m s^{-1} during this time as it exited northeast from the trough axis. A similar evolution occurred at 700 mb with the low closing off at 2870 m over east-central Colorado at 1200 UTC 7 January and the system became vertically aligned by 0000 UTC 8 January.

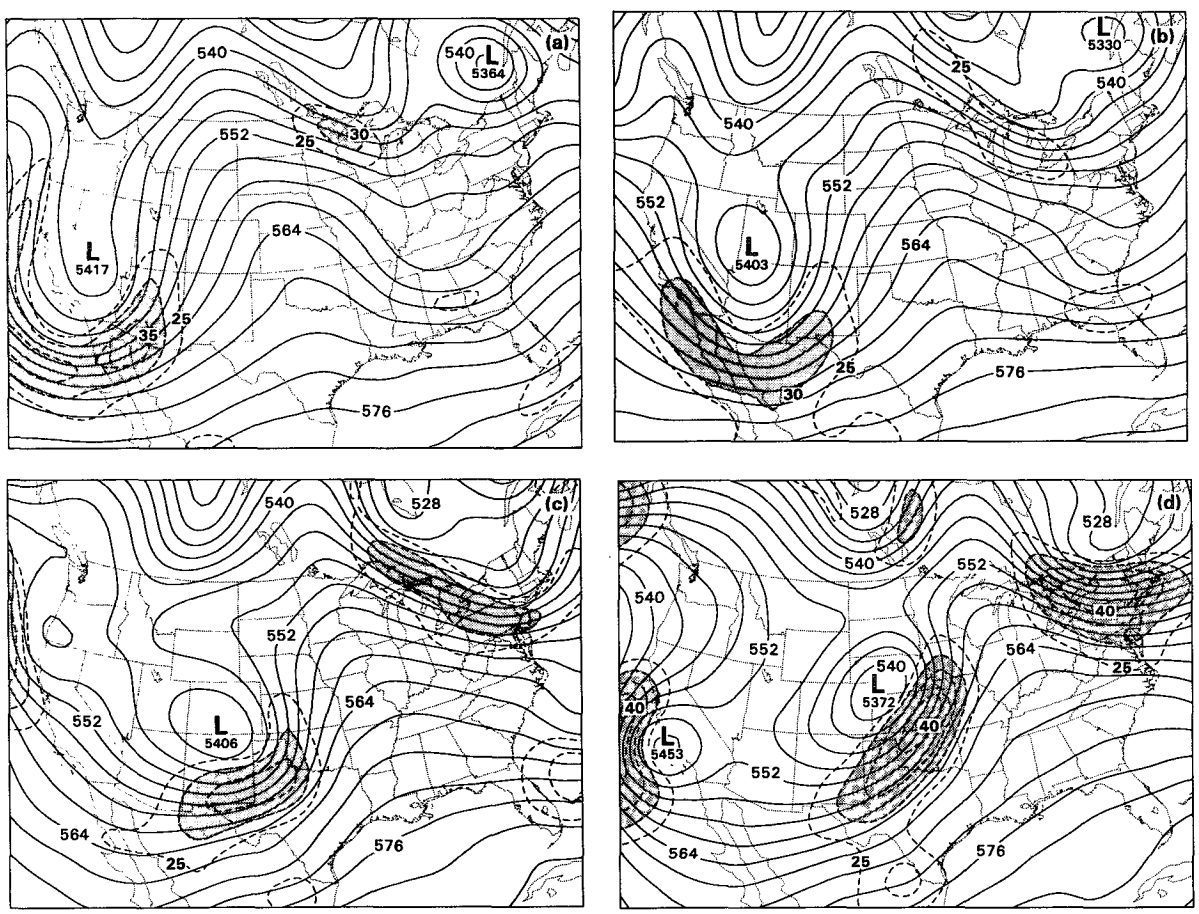

FIG. 4. Nested Grid Model 500-mb height (dam, solid contours) and isotach (m s^{-1}, dashed contours) analyses from (a) 1200 UTC 6 January, (b) 0000 UTC 7 January, (c) 1200 UTC 7 January, and (d) 0000 UTC 8 January 1992. The shaded areas indicate regions with wind speed greater than 30 m s^{-1}.

At 1200 UTC 7 January, a fetch of 700-mb moist air ahead of the trough position extended from south Texas northward through western Oklahoma, Kansas, and Nebraska, and curled westward into northeast Colorado and southeast Wyoming. A dry slot developed from the Mexican Baja Peninsula into central New Mexico. Significant warm advection formed across the Nebraska Panhandle and southeast Wyoming. By 0000 UTC 8 January, the fetch of moist air moved eastward, extending from east Texas through Arkansas and Missouri into Iowa, and westward into Nebraska and South Dakota. The dry slot is collocated with the left rear quadrant of the 700- and 500-mb jet streaks and is positioned across the Texas Panhandle and western Oklahoma. The area of strongest 700-mb warm advection appeared over western Nebraska and western South Dakota. An east–west swath of heavy snow fell across the Nebraska Panhandle into southeast Wyoming, while in Colorado, the heaviest snow fell along a north–south band extending from Greeley (GXY) to the Palmer Lake Divide south of Denver (DEN).

2) MESOSCALE OBSERVATIONS

The focus of this paper is to investigate the north–south band of heavy snow that fell in Colorado where terrain influences are typically important. One might expect from the deep easterly upslope circulation observed with this system that either orographic uplift (e.g., Schlatter et al. 1983) or cold-air damming (e.g., Dunn 1987) would position the region of greatest snowfall along the Front Range and into the Foothills. However, south of Fort Collins (FCL), Colorado, the band of greatest snowfall was observed well east (~40 km) of the mountain barrier, while Front Range communities received snow depths of less than 5 cm.

Examination of the MAPS upper-air and surface analyses begins to provide insight into the possible reasons for the eastward displacement of the observed snowfall. The higher-resolution MAPS analyses show that the upper-level low did not progress smoothly over the Rocky Mountains, but rather redeveloped in the left front quadrant of a secondary, but stronger, jet streak. Figure 5 depicts MAPS 500-mb analyses of height, wind barbs, and isotachs at 3-h intervals from 0600 to 1500 UTC 7 January. At 0600 UTC, the 500-mb low is located over central Utah with a small 15 m s^{-1} jet streak positioned to the northeast. Another more significant jet streak of 25 m s^{-1} is located within the southeast portion of the long-wave trough over eastern New Mexico and southeastern Colorado. By 0900 UTC, the primary low has moved into northeast Utah and the associated jet streak has weakened to less than 15 m s^{-1} over southwest Wyoming. Meanwhile, the stronger jet streak has strengthened to 30 m s^{-1} over southeastern Colorado with indications of a secondary low and associated circulation developing in the left front quadrant over central Colorado. A double low structure with two distinct cyclonic circulations is apparent at 1200 UTC. The primary jet streak has continued to strengthen to greater than 35 m s^{-1} over the Oklahoma and Texas Panhandles. By 1500 UTC, only the new low is apparent over east-central Colorado, with the associated jet streak exceeding 40 m s^{-1} over the Texas Panhandle and western Oklahoma.

The rapid redevelopment of the upper-level low east of the mountain barrier is well correlated with significant surface pressure falls and rapid development of an eastern Colorado cyclone observed during this time period in the surface observations and analyses. MAPS 60-km analyses of mean sea level pressure and 3-h pressure change at 1200 UTC 7 January are presented in Fig. 6a. Earlier MAPS analyses indicate a pressure fall center positioned over south-central Colorado beneath the left front quadrant of the 500-mb jet. At 1200 UTC, a significant 3-h pressure drop of 5.0 mb is located on the Colorado–Kansas border beneath the 500-mb jet left front quadrant, and a low pressure center near the surface is positioned in southeast Colorado. The region of greatest pressure falls moved into western Kansas by 1500 UTC, while the low progressed northeastward to east-central Colorado. Associated with the surface pressure falls is the development of a significant surface cyclone in eastern Colorado. It is important to note that the geostrophic upslope is located primarily in the Nebraska Panhandle and eastern Wyoming, while strong geostrophic northerlies are suggested east of the Colorado mountains.

Actual surface winds show the development of a significant ageostrophic wind component directed into the intensifying cyclone. MAPS 30-km analyses of surface wind and SAO reports at 1200 UTC 7 January (Fig. 6b) suggest a surface low positioned west of Limon (LIC), Colorado, and a significant turning of the wind into the cyclone. Analyzed wind speeds along the Colorado Front Range exceeded 10 m s^{-1} from the west. Significant southeasterly flow over the High Plains has transported low-level moisture northward with the 0°C dewpoint isopleth into the southern Nebraska Panhandle and relatively moist air has wrapped into southeast Wyoming where dewpoints rose 5°C in the previous 6 h. Light snow began at 1100 UTC in Cheyenne (CYS), Wyoming, and at 1000 UTC in Denver, with light rain beginning at 1100 UTC in Colorado Springs (COS).

Later MAPS analyses and surface observations show a well-developed surface cyclone to progress eastward to just southwest of Goodland (GLD), Kansas, by 1900 UTC and then northeastward to southwestern Nebraska by 0000 UTC. Strong westerly flow (15 m s^{-1}) continued over the Continental Divide west of Denver, and the development of strong northwesterly flow was evident from southeast Wyoming into northeast Colorado. Relatively high dewpoints continued to wrap into the cyclone from the northeast, and low dewpoints in northeastern

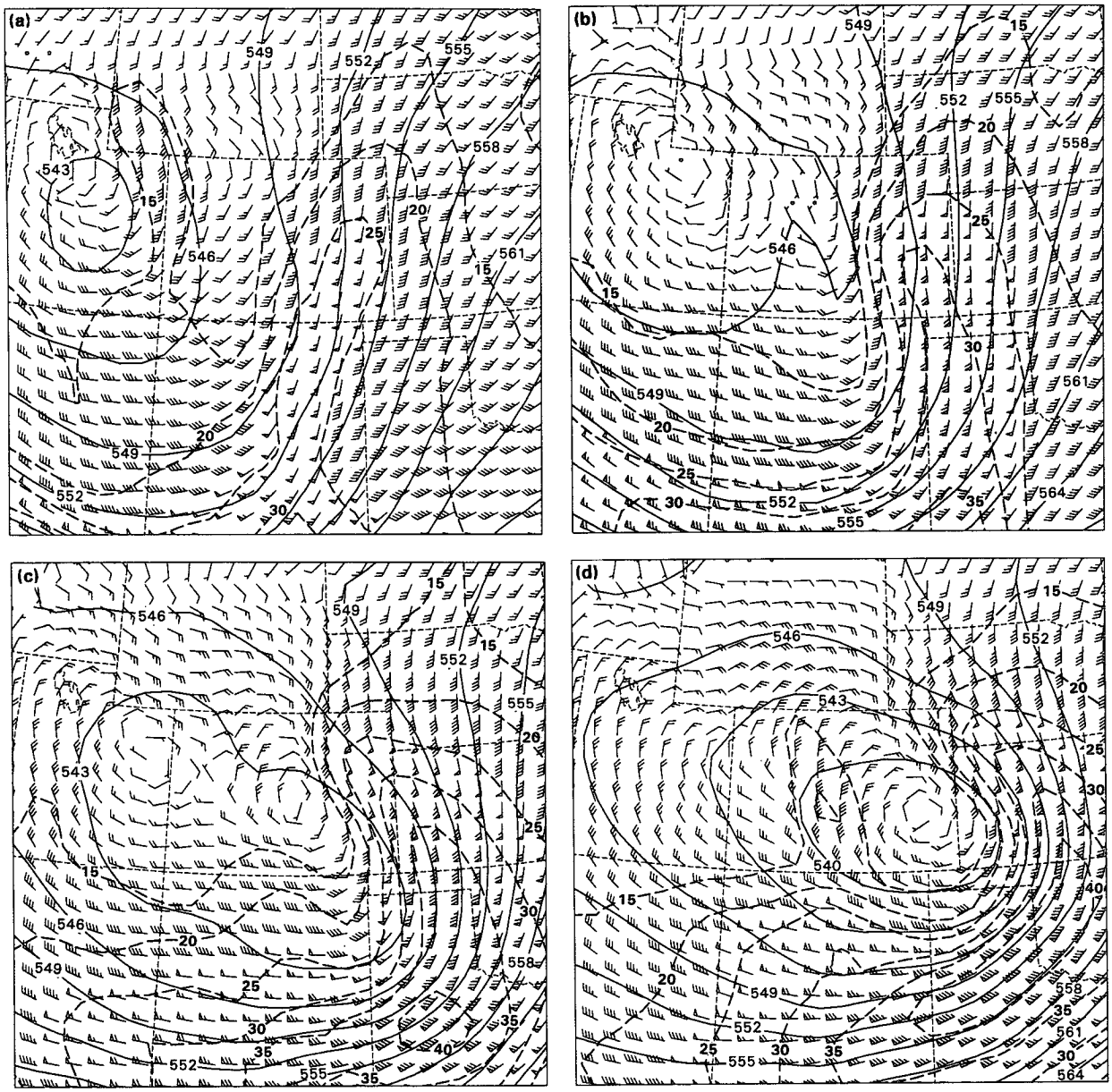

FIG. 5. MAPS 500-mb height (dam), wind barb (one full barb = 5 m s^{-1}), and isotach (m s^{-1}) analyses from (a) 0600 UTC, (b) 0900 UTC, (c) 1200 UTC, and (d) 1500 UTC 7 January 1992.

New Mexico and extreme southern Colorado suggest the location of the dry slot and downward mixing. Winds at Cheyenne remained northwesterly throughout the event and were quite strong during the afternoon with gusts exceeding 20 m s^{-1}. Winds were also northwesterly at Denver through 2000 UTC, an unusual direction for heavy snow due to the downslope component near the surface. After 2000 UTC, the winds shifted to north and northeast with the velocity increasing to greater than 15 m s^{-1} and gusts reaching 20 m s^{-1}.

Rawinsonde observations from Denver, North Platte, Nebraska, and Lander, Wyoming (not shown), indicated a near-saturated environment up to at least 500 mb and a stable layer between the surface and 700 mb. The combination of the stable layer, strong northwesterly flow over the Cheyenne Ridge, and a northeast wind at Denver suggests favorable conditions for the development of an anticyclonic circulation, known as the Longmont anticyclone (Young and Johnson 1984), that forms in the lee of the west-to-east elevated terrain

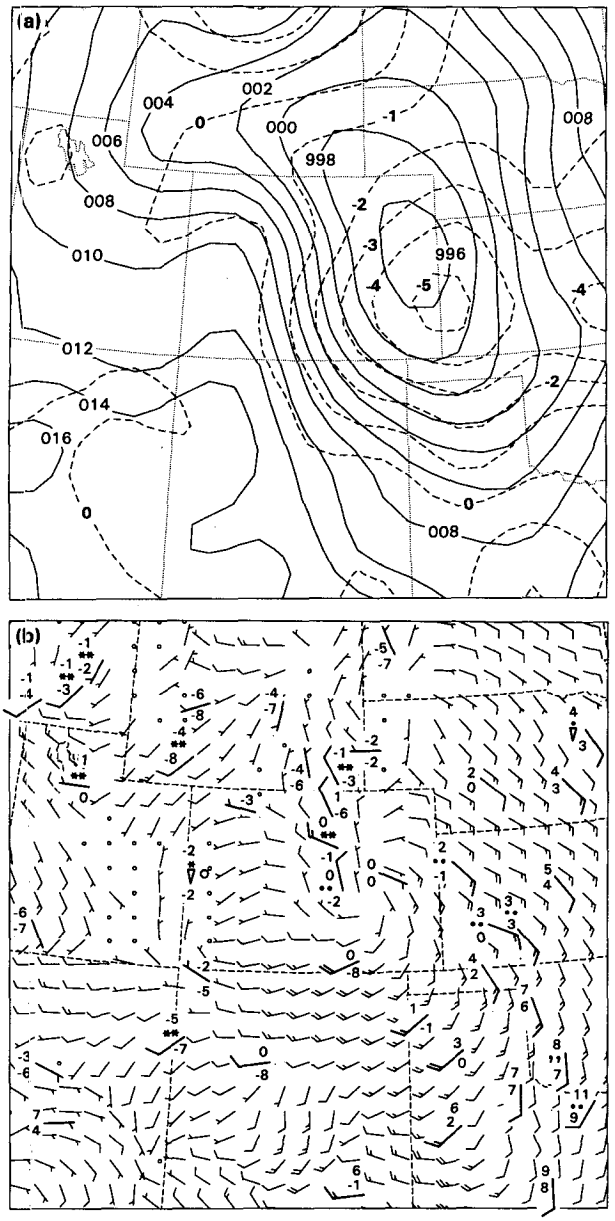

FIG. 6. MAPS 1200 UTC 7 January 1992 analyses of (a) mean sea level pressure (mb, solid contours) and 3-h pressure change (mb, dashed contours) and (b) surface wind barb (one full barb = 5 m s^{-1}) with SAO reports (temperatures and dewpoints are in °C).

between Fort Collins, Colorado, and Cheyenne, Wyoming.

3) LOCAL-SCALE OBSERVATIONS

Examination of Doppler radar, wind profiler data, and automated surface observations provides an even closer view of the cyclone development and associated wind flow. Reflectivity data from a Doppler radar (Fig. 7) located approximately 10 km northeast of Denver provide an indication of the areal extent, intensity, and evolution of the snowfall. At 1200 UTC, the highest radar reflectivity was located along the foothills at which time these locations received light amounts of snow. By 1500 UTC, however, the north–south band of heavy snow, indicated by the region of reflectivity exceeding 25 dBZ centered along a line stretching from east of Fort Collins, across Denver, and southeast to the Palmer Lake Divide, had moved eastward away from the mountain barrier. A band of low reflectivity is observed between the mountain barrier and the heavy snow band. This basic pattern continued through 0000 UTC 8 January with a decrease in areal coverage near the end of the period.

The Platteville, Colorado, wind profiler, located along the western edge of the heavy snow band, depicts three distinct flow regimes in the vertical (Fig. 8). A layer of low-level north-northwest winds expanded up to 4 km by 1800 UTC. A middle layer of mostly east winds increased in depth with time. At 1800 UTC, the easterlies were observed between 4 and 11 km. Upper-layer winds were mostly from the south and veered with time in response to the eastward movement of the long-wave trough. After 1800 UTC, the midlayer easterlies shifted to near northerly by 0000 UTC, resulting in a deep layer of northerlies up to 10.5 km. Prior to 1800 UTC, the ascent of the easterly flow over the low-level northerlies was a likely contributor to the heavy band of observed snowfall. However, areas of moderate to heavy snow continued after 1800 UTC with strong winds from the north.

Midlevel easterlies above low-level northerlies often indicate a cold-air damming situation (e.g., Dunn 1987). However, observations from the FSL mesonet (Fig. 7) indicate that strong west winds persisted through the entire event in the mountain (western) stations, warmer temperatures occurred adjacent to the Front Range, and there was no easterly flow in the eastern portion of the domain, all indicators that this is not a cold-air damming case. Another interesting aspect of the mesonet observations is the development of light northeasterlies adjacent to the Front Range. With strong northwest flow observed by the northern stations, the mesonet indicates a Longmont anticyclone regime as mentioned previously. However, unlike other cases where precipitation develops along the Front Range on the convergence line between the northwesterlies and the northeasterlies (e.g., Wesley 1991), the heavy snow fell farther east. The heavy snow actually fell within a region of observed strong northwesterly flow that increased significantly with time. Doppler radar velocity data (not shown) also indicated the development of strong (25 m s^{-1}) north-northwest flow collocated with the band of heavy snow.

4) SUMMARY

The synoptic-scale observations indicate that the 7 January 1992 blizzard had many characteristics of a

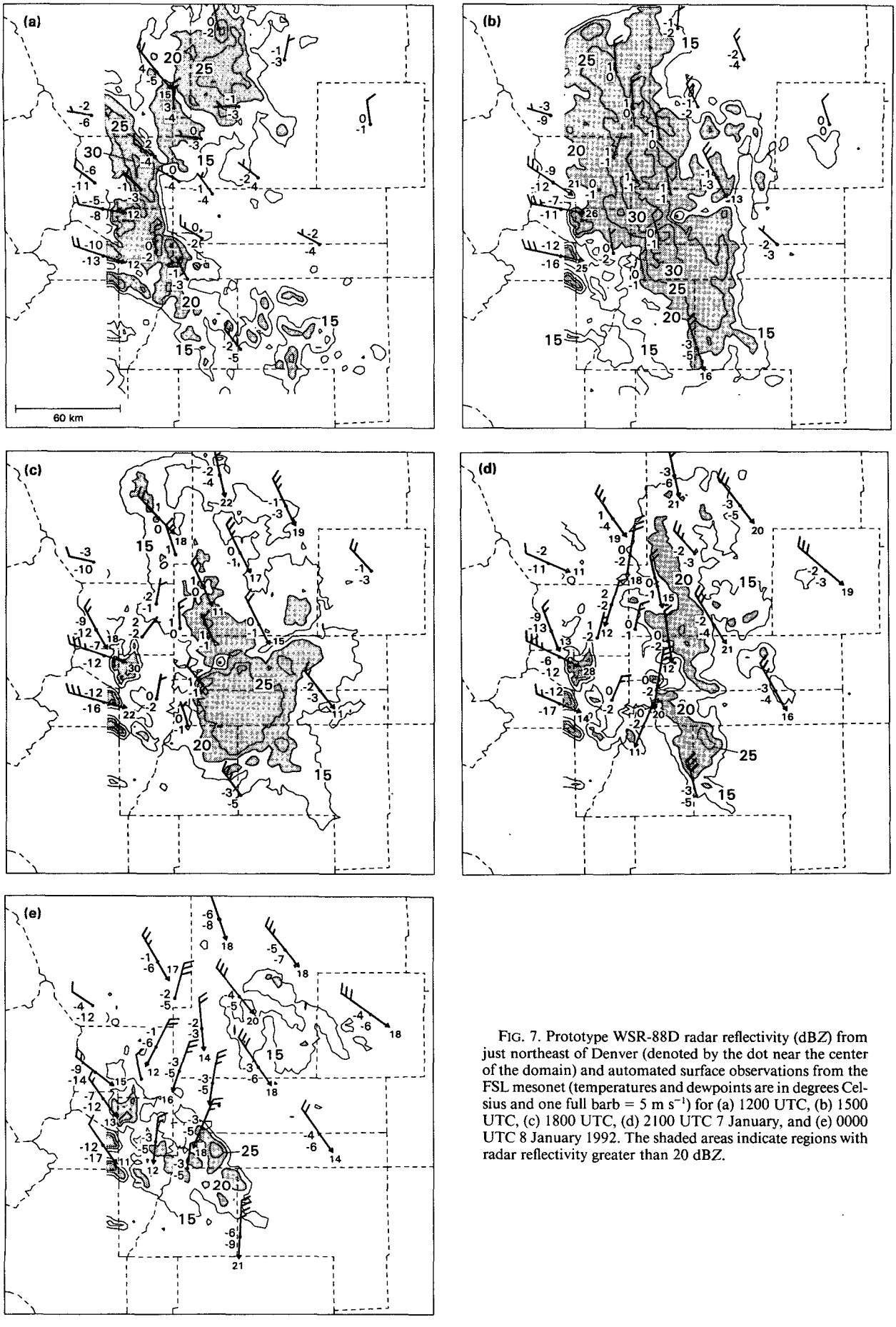

FIG. 7. Prototype WSR-88D radar reflectivity (dBZ) from just northeast of Denver (denoted by the dot near the center of the domain) and automated surface observations from the FSL mesonet (temperatures and dewpoints are in degrees Celsius and one full barb = 5 m s^{-1}) for (a) 1200 UTC, (b) 1500 UTC, (c) 1800 UTC, (d) 2100 UTC 7 January, and (e) 0000 UTC 8 January 1992. The shaded areas indicate regions with radar reflectivity greater than 20 dBZ.

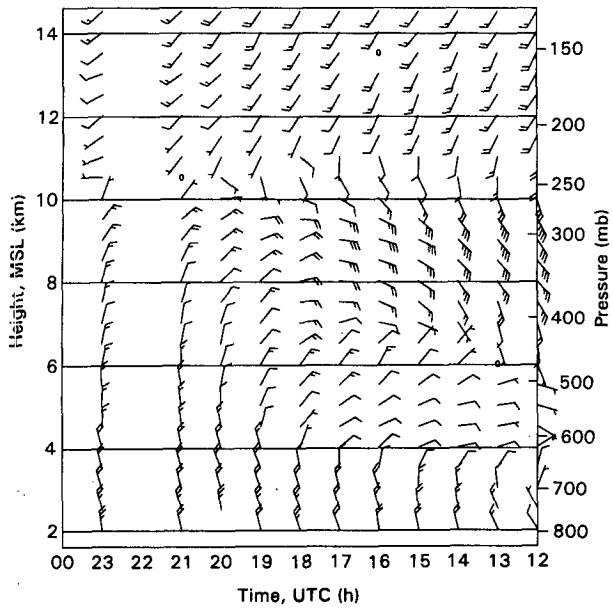

FIG. 8. Time-height series of wind (one full barb = 5 m s^{-1}) from the Platteville, Colorado, wind profiler for 1200 UTC 7 January to 0000 UTC 8 January 1992.

deep cyclonic, upslope circulation storm (Reinking and Boatman 1986). However, two aspects of the storm were unusual: 1) the development of strong westerly lower-tropospheric flow east of the Continental Divide, and 2) the eastward displacement of greatest snowfall away from the mountain barrier. Significant pressure falls observed over the eastern plains are well correlated with the redevelopment of the upper-level low east of the mountain barrier. The isallobaric effect of the pressure falls probably contributed to the development of an ageostrophic wind component directed into the developing cyclone and the formation of the strong westerly surface flow observed east of the Continental Divide. Since westerly downslope flow is typically warmer and drier, this feature likely contributed to the warmer temperatures and low amounts of snowfall observed along the Front Range.

b. Model simulations

The observations of 7 January 1992 indicate several interesting mesoscale features including: 1) persistent strong downslope flow east of the mountain barrier crest, 2) the development of weak northeasterlies adjacent to the Front Range, 3) the generation of strong northwesterlies at the surface and low levels over the eastern plains, and 4) the eastward displacement of greatest snowfall away from the mountain barrier. To determine if the mesoscale model forecasts can resolve these features and provide further meteorological insight as to their existence, the RAMS mesoscale model is initialized with real-time 10-km grid increment LAPS analyses from 1200 UTC 7 January 1992. Twelve-hour forecasts were completed using identical model physics, except for the LMIC simulation, which uses the RAMS explicit representation of microphysics option.

1) LSFC SIMULATION—RAMS INITIALIZED WITH LAPS

The LSFC simulation is initialized with the 10-km grid interval LAPS mass, wind, and moisture analyses. The separate LAPS surface analysis is also blended into the model initialization. A comparison of the low-level [146 m above ground level (AGL)] RAMS forecast winds with surface aviation wind observations (SAO, Fig. 9), FSL mesonet reports (Fig. 7), and LAPS surface analyses (Fig. 10) indicates that the model simulation developed the important mesoscale surface features. At 1500 UTC, the 3-h forecast shows westerly ridge-top winds west of Denver have strengthened to 25 m s^{-1}, while weak northeasterlies have developed along the Front Range, both of which compare favorably with the SAOs, mesonet observations, and LAPS objective analysis. Some minor differences are noted in the location and structure of the cyclonic surface circulation. The model indicates a stronger surge of westerly flow in southern Colorado than is indicated by the LAPS analysis. The discrepancies may be partially accounted for by the difference in elevation between the LAPS surface analysis (10 m AGL) and the RAMS forecast (146 m AGL), which can be expected to be greater in the morning prior to full mixing of the boundary layer.

The 6-h RAMS forecast (1800 UTC) shows continued strengthening of the westerly ridge-top winds to 30 m s^{-1} and an area of weak northeasterly flow north and west of Denver, consistent with observations. Over the eastern plains, the LAPS analysis depicts the surface cyclone as a north–south elongated shear line extending from Akron (AKO) southward to west of Lamar (4LJ). A similar shear line is predicted by RAMS and is located approximately 30 km west of the LAPS analyzed shear line. It is difficult to ascertain the exact location and structure of the shear line due to the sparsity of data in this region. However, both the RAMS forecast and LAPS analysis show close agreement with the available observations. Two regions of strong winds observed in LAPS and forecast by RAMS are northerlies over the Cheyenne Ridge and northwesterlies over the Palmer Lake Divide west of Limon. The model continues to predict strong westerly flow south of the surface cyclone.

RAMS continues to forecast strong westerly ridge-top winds at 2100 UTC with a slight decrease in magnitude to 25 m s^{-1}. RAMS winds adjacent to the Front Range and north of Denver are northeasterly, similar to the observed winds at several of the mesonet stations. High winds ($\sim$20 m s^{-1}) in RAMS continue over the Cheyenne Ridge and the Palmer Lake Divide that

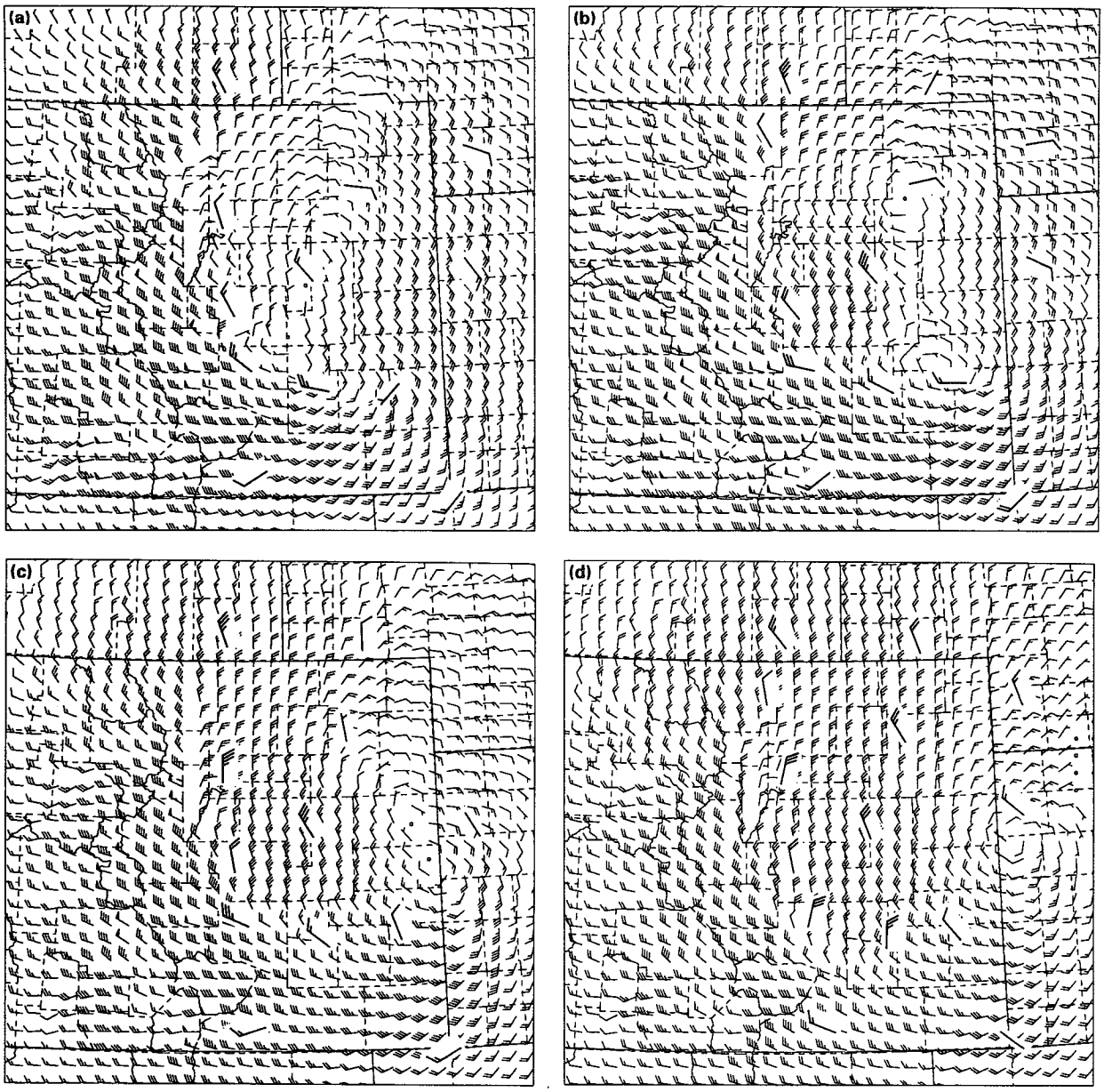

FIG. 9. RAMS (LSFC) low-level (146 m AGL) wind (one full barb = 5 m s^{-1}) predictions and actual SAO wind reports (large barbs) at model validation time from (a) the 3-h forecast valid at 1500 UTC, (b) the 6-h forecast valid at 1800 UTC, (c) the 9-h forecast valid at 2100 UTC 7 January, and (d) the 12-h forecast valid at 0000 UTC 8 January 1992. Wind barbs are displayed at every other grid point.

compare favorably with LAPS analyses and observations. The structure of the surface cyclone, located near the Colorado–Kansas border, is similar in both RAMS and LAPS; however, the RAMS forecast position is about 20–30 km southeast of the LAPS position. Again, the exact location of the low is difficult to ascertain because of the sparsity of data in this region.

RAMS 12-h forecast winds at 0000 UTC indicate a backing and weakening of the winds over ridge top whereas north-northeast winds are predicted in the Denver area. Strong north-northwest flow is forecast west of the surface cyclone. The center of the RAMS cyclonic circulation is located approximately 30 km southwest of Goodland and is about 100 km south of the LAPS analyzed position.

The RAMS forecasts have developed the essential surface mesoscale features of this system. Persistent strong downslope flow east of the barrier crest is predicted. The development of north-westerly flow over the Cheyenne Ridge and northeasterly flow adjacent to the Front Range is consistent with observations and appears to have the general characteristics of a Long-

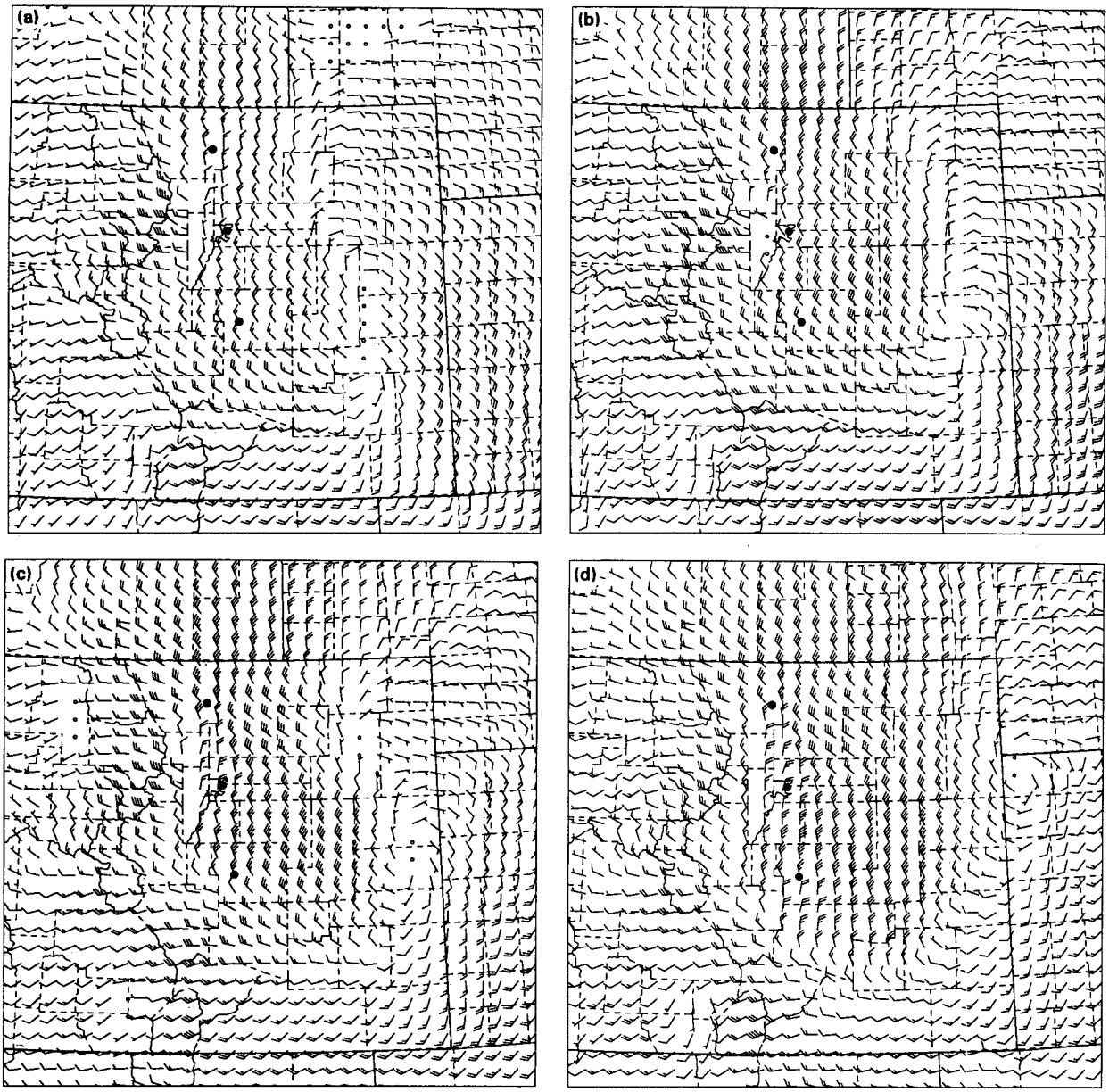

FIG. 10. LAPS surface wind (one full barb = 5 m s^{-1}) analyses from (a) 1500 UTC, (b) 1800 UTC, (c) 2100 UTC 7 January, and (d) 0000 UTC 8 January 1992. Wind barbs are displayed at every other grid point. Solid dots indicate the locations of Fort Collins, Denver, and Colorado Springs, from north to south.

mont anticyclone. The model successfully forecast the development of strong north-northwest flow over the eastern plains that created the severe blizzard conditions in this region.

Upper-air features of the cyclone also appear to be well predicted by the model simulation. A comparison of RAMS upper-air forecasts interpolated from the model σ_z surfaces to isobaric surfaces with MAPS upper-air analyses indicates a similar structure and evolution of the upper-level cyclone. The 500-mb height forecasts indicate a positive bias with differences of 10–15 m at 3 h, increasing to 20–40 m by 12 h. As expected from a prediction using a 10-km grid increment, significantly more mesoscale information is offered by RAMS. However, it is very difficult to validate this information given the sparsity of upper-air observations and the coarser 60-km grid increment MAPS analyses.

The Platteville wind profiler was the sole instrument available during this case that provided high temporal resolution upper-air observations (Fig. 8). Comparing a time series of RAMS upper-air wind forecasts from the nearest model grid point to Platteville (Fig. 11)

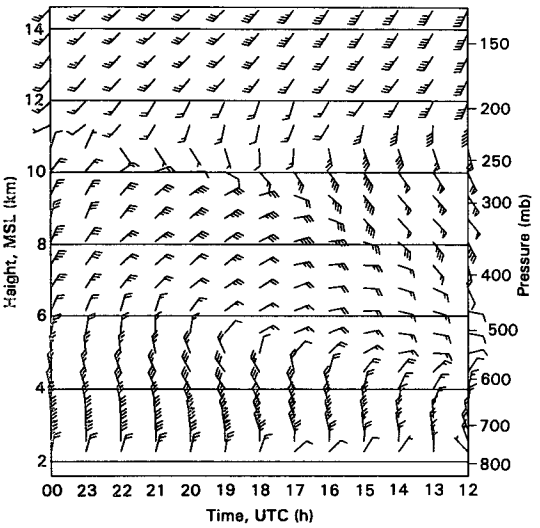

FIG. 11. Time-height series of RAMS (LSFC) forecast wind (one full barb = 5 m s^{-1}) for the model grid point closest to Platteville, Colorado, from the 0- to 12-h prediction valid at 1200 UTC 7 January through 0000 UTC 8 January 1992.

with the wind profiler observations provides a glimpse of the mesoscale accuracy of the RAMS upper-air predictions. The RAMS predictions clearly define the three distinct flow regimes in the vertical observed by the Platteville wind profiler. The temporal evolution of the low-layer northerlies as they expand upward and the midlayer easterlies backing to northerly is well forecast by RAMS. The depth of the flow regimes and the interfaces between each regime (e.g., the weaker winds near 11 km from 2100 to 0000 UTC) is very realistic. The lowest-level winds (below the first available gate in the wind profiler) from 1300 to 1700 UTC depict the northeasterly flow associated with the Longmont anticyclone regime.

A band of moisture wrapping around the cyclone and moving into the Front Range from the northeast is indicated by the RAMS forecasts (not shown). The 3-h forecast (valid at 1500 UTC) shows a mixing ratio maximum of 6 g kg^{-1} over northeast Colorado. The maxima progresses westward to northcentral Colorado by 6 h (1800 UTC), southward across Greeley and Denver at 9 h (2100 UTC), and farther south to near Colorado Springs by 12 h (0000 UTC). The band of moisture appears to be well correlated with the observed snowfall over the eastern plains. However, much of the heavy snow observed from Fort Collins to Denver fell prior to the arrival of greatest moisture.

Although the moisture adjacent to the Front Range may have been initially limited, the observed heavy snow band appears to be well correlated with a region of significant upward vertical motion. RAMS forecasts of maximum vertical motion indicate a persistent north–south band of upward vertical motion to exist from Fort Collins to south of Denver (DEN). The 3-h forecast (Fig. 12) shows the band to exceed 0.5 m s^{-1} and strengthens to greater than 0.75 m s^{-1} by 6 h (not shown). The maximum upward vertical motion band moves southward by 9 h and is primarily south of Denver at 12 h. The location and movement of the predicted band of upward vertical motion corresponds well with the Doppler radar reflectivity (Fig. 7).

A three-dimensional view of the moisture and vertical velocity shows the band of moisture to be a low- to midtropospheric feature (~700–600 mb) that is sloped from northeast to southwest, while the band of upward vertical motion appears to be closely associated with the development of a mountain wave east of the Continental Divide. A representative sample of vertical cross sections illustrates these features. A west–east vertical cross section (located approximately 20 km north of Denver) of RAMS forecast potential temperature at 3 h (Fig. 13a) indicates a weakly developed mountain wave east of the barrier. The mountain wave appears to be confined to the lower troposphere, within a layer of relatively stable air below 6 km. A layer of less stable air is indicated above 6 km, resulting in a static stability profile that decreases with height. This type of two-layer atmospheric configuration supports the generation of a trapped wave system (Scorer 1949; Smith 1979). Hence, the development and maintenance of the mountain wave is likely due to this trapped wave process.

Descent exceeding 1.0 m s^{-1} is indicated in the western portion of the wave (Fig. 13b). A maximum of upward vertical motion is predicted east of the

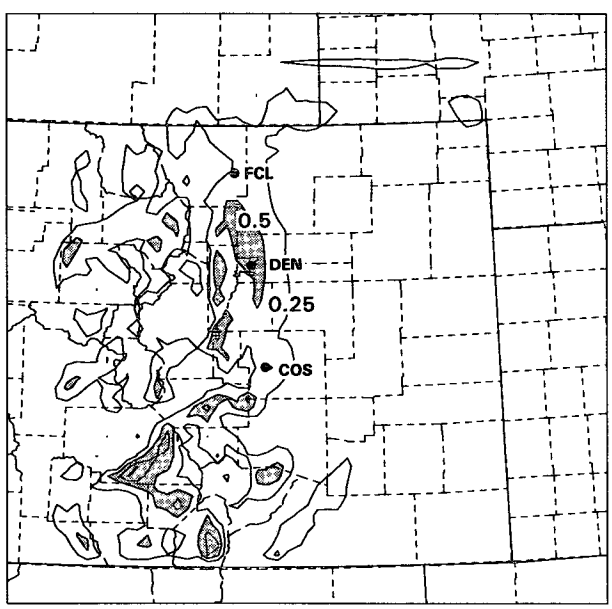

FIG. 12. RAMS (LSFC) maximum upward vertical motion (m s^{-1}) prediction from the 3-h forecast valid at 1500 UTC 7 January 1992. Contour interval is 0.25 m s^{-1}. The shaded areas indicate regions of upward vertical velocity exceeding 0.5 m s^{-1}.

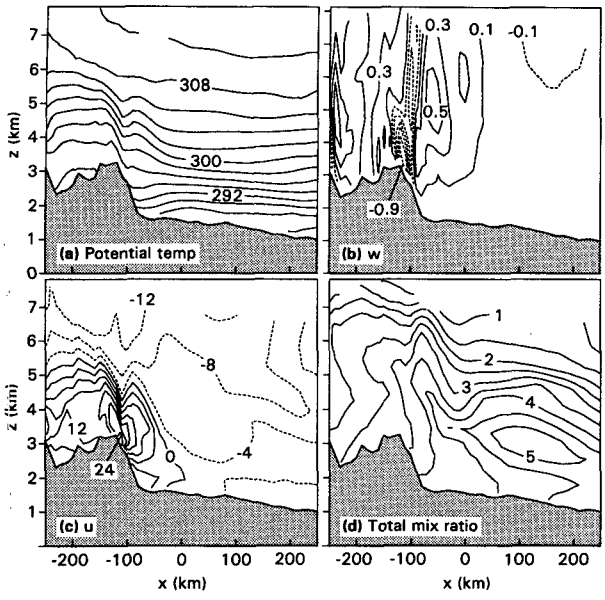

FIG. 13. West–east vertical cross sections from RAMS (LSFC) 3-h forecast valid at 1500 UTC 7 January 1992 of (a) potential temperature (K), (b) upward vertical motion (m s^{-1}, contour interval = 0.2 m s^{-1}), (c) u-component wind (m s^{-1}, contour interval = 4.0 m s^{-1}), and (d) total mixing ratio (g kg^{-1}, contour interval = 0.5 g kg^{-1}). Cross section location is approximately 20 km north of Denver.

mountain barrier. The lower portion of the ascent region (0.4 m s^{-1}), located at 3.5 km, is positioned in the eastern area of the mountain wave. The upper ascent (0.6 m s^{-1}) region is located at 5 km and appears to be the result of easterly flow (Fig. 13c) rising up and over the wave-perturbed flow. This is consistent with the midlayer easterly flow observed at 1500 UTC by the Platteville wind profiler (Fig. 8). Total mixing ratio suggests a band of moisture rising from east to west in association with the easterly flow (Fig. 13d).

The 6-h RAMS predictions indicate amplification of the mountain wave with potentially warmer air progressing down the barrier creating a baroclinic zone adjacent to the Front Range, consistent with temperature observations by the FSL mesonet. Downward vertical motion associated with the mountain wave has progressed down to the base of the barrier. A double upward vertical motion maximum continues to be predicted, but the lower maxima near 3 km (0.45 m s^{-1}) is now stronger than the upper maxima near 5 km (0.2 m s^{-1}). Model predicted u-component flow shows the westerly component wind to extend further out onto the plains at this time and to be greater in depth adjacent to the Front Range. The result is weaker easterly component flow rising over the mountain wave and hence weaker upward vertical motion at 5 km. These predictions are consistent with the observed Platteville profiler winds between 4 and 6 km that backed from east to northeast between 1500 and 1800 UTC. The predicted total mixing ratio continues to indicate relatively moist air rising above the mountain wave from the east, and low-level drying is suggested east of the barrier in conjunction with the downward motion.

The mountain wave continues to be evident in the 9-h predicted potential temperature field with a further enhancement of the baroclinic zone adjacent to the Front Range. Downward vertical motion remains in the western portion of the wave, while upward vertical motion (0.45 m s^{-1} near 3 km) is depicted only within the eastern region of the wave. A westerly component to the flow occupies nearly the entire cross section below 5 km, consistent with the Platteville profiler observations. Easterly component flow forecast above 5 km appears to be too high to be forced upward by the mountain wave; hence, the second, higher upward vertical motion maxima is no longer evident. The development of a significant northerly component jet core (20 m s^{-1}) is indicated adjacent to the Front Range in association with the baroclinic zone observed in the potential temperature field.

The wave amplitude has decreased in the 12-h forecast of potential temperature, while the baroclinic zone adjacent to the Front Range remains in place. The downward/upward vertical motion couplet is indicated within the wave. Strong westerly component flow continues in the lee of the barrier except for a small area of easterly component adjacent to the barrier, consistent with the northeasterly surface observations in the FSL mesonet.

2) LMIC SIMULATION—A FULL MICROPHYSICS PREDICTION

The LSFC simulation provides a mesoscale representation of the mass, wind, and moisture structure of the 7 January 1992 blizzard. With the addition of liquid and ice phase microphysics to the LSFC simulation, precipitation processes and their effects on other processes can be investigated.

Significant differences are not indicated between the mass and wind fields of the LSFC and LMIC simulations. Low-level (146 m AGL) wind forecasts from the LMIC simulation indicate a similar structure and evolution of the surface cyclone. The LMIC simulation develops significant westerly flow over the mountains west of Denver and strong northwesterly flow west of the surface cyclone, similar to the LSFC simulation. Minor differences are noted in the structure of the flow north of Denver at 1800 UTC where the LSFC simulation shows northeasterly flow (Fig. 9b), while the LMIC simulation indicates north-northwesterly flow, closer to the FSL mesonet observations (Fig. 7c).

The LMIC predictions of maximum upward vertical motion (not shown) are similar to the LSFC forecasts (Fig. 12) for the Fort Collins-to-Denver band, but differences are noted over the northeast plains of Colorado. The 3-h forecasts of vertical motion indicate that

the magnitude and shape of the upward vertical motion band adjacent to the Front Range are very close. However, two significant southwest–northeast-oriented bands (>0.75 m s^{-1})—one east of Cheyenne and the other northeast of Akron—are evident in the LMIC simulation but are not predicted in the LSFC simulation. The LSFC simulation includes the effects of diabatic heating that results from vapor condensation to liquid, but conversion to ice is not accounted for. Hence, the additional diabatic heating effects of liquid to ice must be contributors to the stronger predicted upward vertical motion in the LMIC simulation. A similar result is observed in the 6-h forecasts with the region of greater than 0.25 m s^{-1} upward vertical motion extending from Denver northeastward into the Nebraska Panhandle. At 9 and 12 h, the two simulations are quite close again with the LMIC prediction showing the dissipation of significant ascent over the northeast plains.

Representative west–east vertical cross sections provide an indication of the precipitation processes occurring. Three-hour predictions of potential temperature and vertical motion (not shown) indicate a mountain wave to the east of the higher terrain and a downward/upward vertical motion couplet, similar to the LSFC simulation (Fig. 13). Recall that the upward vertical motion appears to be the result of rising motion in the wave near 3.5 km and lifting of easterly flow over the wave near 5 km. A tall (5 km) vertical column of snow is collocated with the region of upward vertical motion and a maximum of aggregates is positioned in the lower half of the column (Fig. 14). The regions of greatest snow and aggregates at the surface are displaced slightly east of the mountain barrier with the total quantity decreasing westward up the Front Range. Two factors are likely contributors to the decreased Front Range snow: 1) snow that might fall into the region of downward vertical motion over the Front Range will quickly sublimate (and probably act to accentuate the downward motion) and 2) the strong low-level westerly flow tends to blow the snow eastward over the plains.

The 6-h forecast of snow mixing ratio (Fig. 14) is again correlated with the regions of ascent and aggregates are maximized below the areas of greatest snow mixing ratio. A narrow dry zone with no snow or aggregates is depicted over the Front Range in association with the dry region of descent in the western portion of the wave. The extension of the westerly component flow over the plains suggests that snow and aggregates are carried eastward, and hence the predicted broadening in the vertical columns of snow and aggregates. The regions of greatest surface snow and aggregates are now displaced approximately 40 km east of the barrier.

The 9-h forecast indicates the columns of greatest snow and aggregates east of the Front Range are confined below 4 km with an eastward extension. The dry slot continues over the Front Range and significant westerly component flow likely creates the eastward extension. Surface snow and aggregates concentrations continue to be greatest at about 40 km east of the mountain barrier with some decrease in magnitude. At 12-h, snow and aggregates east of the Front Range are primarily confined to the lowest 1 km AGL, and the concentrations have decreased significantly in magnitude. Greatest surface amounts of snow and aggregates are located about 30 km east of the barrier.

The microphysics version of RAMS generates a quantitative precipitation forecast. The 12-h forecast of melted precipitation (Fig. 15) indicates that the model is capable of resolving the mesoscale variation that was observed (Fig. 3). The observed snow to melted water ratio was about 15:1, hence an observation of 30 cm of snow is equivalent to approximately 20 mm of melted precipitation. The north–south band of model-predicted precipitation from Greeley to south of Denver agrees well with the observed band in location and magnitude. Other features predicted by RAMS that correspond well with the observations include the dry zones along the Front Range and around Colorado Springs, the westward extension of maximum precipitation from Fort Collins to the Continental Divide, the east–west band of precipitation from southeast Wyoming to the Nebraska Panhandle, and the overall coverage of the greater than 4 mm precipitation area.

c. Comparison to operational forecasts

A qualitative comparison of the RAMS simulations with other operational models helps to answer one of the objectives of this paper: can a mesoscale numerical model initialized with high-resolution, nonhomogeneous data detect mesoscale features and add value to currently available regional scale model forecasts. The LMIC simulation is compared to operational predictions from NMC's NGM and FSL's MAPS models.

The 6-h MAPS forecast of surface winds (Fig. 16) shows the cyclone position to be in east-central Colorado, close to the RAMS predicted position (Fig. 9) and the LAPS analyzed location (Fig. 10), while the NGM 6-h forecast (Fig. 17) positions the low a little farther east near the Kansas border. The RAMS forecast provides greater mesoscale detail especially over the mountains with 30 m s^{-1} predicted wind speeds compared to 15 m s^{-1} in the MAPS forecast, and adjacent to the Front Range where RAMS predicts northeasterlies as observed in the FSL mesonet. The RAMS forecast suggests stronger northwest flow than MAPS west of the surface cyclone, which appears to be in closer agreement to the Limon SAO.

Both the 12-h MAPS and NGM forecasts position the surface cyclone in west-central Kansas, a little south of the LAPS analyzed location on the western Kansas–Nebraska border. The RAMS forecast position is also south of the analyzed location, but closer than the MAPS and NGM forecasts. Recall that the MAPS forecast is the nudging target for the RAMS lateral

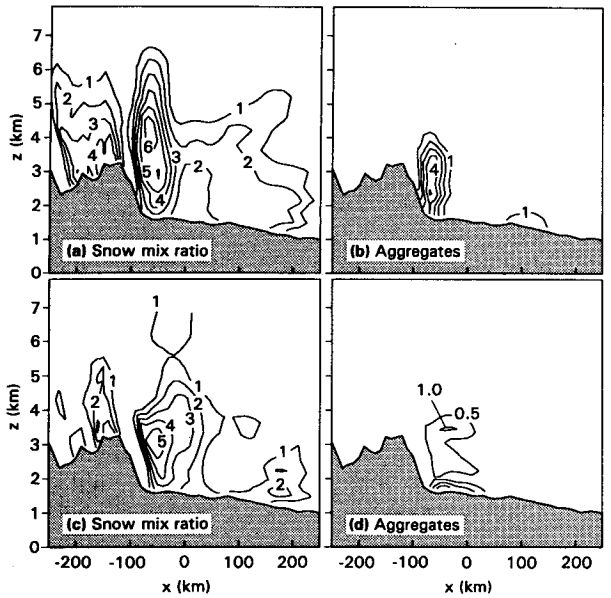

FIG. 14. West–east vertical cross sections from RAMS (LMIC) 3-h forecast valid at 1500 UTC 7 January 1992 of (a) snow mixing ratio (g kg^{-1}, contour interval = 0.1 g kg^{-1}, 1 unit = 0.1 g kg^{-1}) and (b) aggregate mixing ratio (g kg^{-1}, contour interval = 0.1 g kg^{-1}, 1 unit = 0.1 g kg^{-1}), and 6-h forecast valid at 1800 UTC of (c) snow mixing ratio (g kg^{-1}) and (d) aggregate mixing ratio (g kg^{-1}). Cross section location is approximately 20 km north of Denver.

boundary condition that probably influenced the RAMS forecast position. The RAMS 12-h forecast surface winds provide a closer agreement to observations than either MAPS or NGM with the strong, but weakening, northwest flow over the mountains, the northeasterly flow adjacent to the Front Range, and the strength of the northwesterly flow west of the surface cyclone.

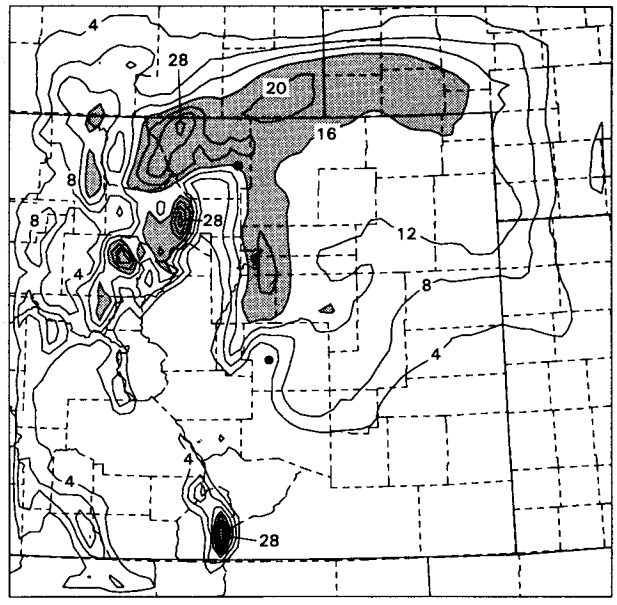

FIG. 15. RAMS (LMIC) 12-h melted precipitation (mm) forecast. The shaded areas indicate regions with precipitation greater than 16 mm.

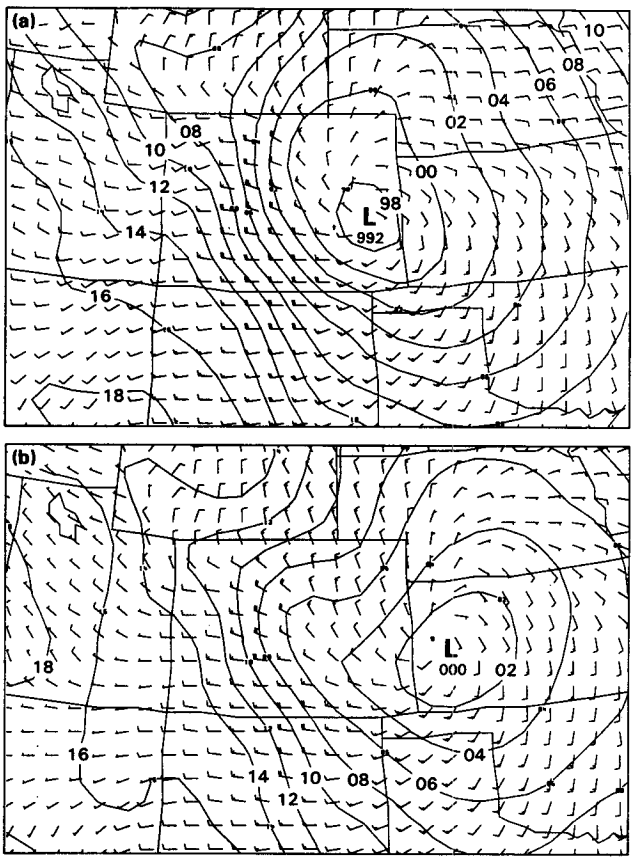

FIG. 16. MAPS mean sea level pressure (mb) and surface wind (one full barb = 5 m s^{-1}) predictions from (a) the 6-h forecast valid at 1800 UTC 7 January and (b) the 12-h forecast valid at 0000 UTC 8 January 1992.

The 12-h NGM precipitation forecast (Fig. 18) indicates a large swath of greater than 0.64-cm (0.25 in.) melted water from northeast Colorado, across western Nebraska, and into southcentral South Dakota. The model appears to have predicted a quasigeostrophically forced area of precipitation typically observed north-northwest of the surface low center (Fawcett and Saylor 1965) that was observed across southeast Wyoming and the Nebraska Panhandle. There is, however, no suggestion of any mesoscale structure within the forecast precipitation swath. The MAPS 3- and 6-h precipitation forecasts (Fig. 19) valid at 1500 and 1800 UTC indicate a northwest-southeast band of heavy precipitation over and east of the northern and central Colorado mountains. Compared to the NGM, MAPS appears to have provided an improved prediction of the observed heavy snow east of the Colorado Front Range, but MAPS was still unable to resolve the me-

soscale structure of the dry band observed along the Front Range. The higher-resolution LMIC precipitation forecast suggests that RAMS is capable of resolving the dry band (Fig. 15). This capability, combined with the enhanced forecasts of surface winds, suggests that the RAMS predictions are capable of adding significant value to the currently available short-range (0–12-h) operational forecasts.

5. Discussion and conclusions

Two objectives of this paper are to evaluate the accuracy of forecasts from a mesoscale numerical model initialized with high-resolution, nonhomogeneous data and determine if the model forecasts can resolve mesoscale features, thus adding value to currently available national domain model predictions. The RAMS numerical model was initialized with high-resolution (10-km horizontal grid interval) operational LAPS analyses for a significant Colorado Front Range snowstorm that occurred on 7 January 1992. The storm is ideal for this investigation since observations contained strong winds, heavy snowfall, and significant mesoscale precipitation variation.

An unusual aspect of the 7 January snowstorm was the observed band of heavy snow (20–40 cm) that fell along a north–south line approximately 40 km east of the Front Range mountain barrier, while the barrier itself received less than 5 cm of snowfall. Significant mesoscale variation was also observed in the surface winds with strong, westerly downslope flow over the Front Range, weak northeasterly flow adjacent to the Front Range, and strong north-northwest flow over the eastern plains that generated blizzard conditions for most of the day. Although the associated convergence zone between the westerlies and northeasterlies has been correlated with bands of enhanced snowfall in other storms, the heavy snow band with this system fell farther east in the region of strong north-northwesterly flow.

The RAMS model simulations were successful in resolving most of the pertinent observed mesoscale features. In general, the surface flow characteristics were well predicted. The 7 January simulations resolved the three major surface wind regimes including 1) the persistent strong downslope flow east of the mountain barrier crest, 2) the development of weak northeasterlies adjacent to the Front Range, and 3) the generation of strong northwesterlies at the surface and low levels over the eastern plains. Although difficult to verify, the model predictions appeared to resolve the upper-air mesoscale flow features. Time series comparisons of upper-level model forecast winds with wind profiler observations showed excellent agreement. Precipitation forecasts from the microphysics simulation were capable of accurately resolving mesoscale features. The simulations were successful at predicting the eastward displacement of greatest snowfall away from the mountain barrier.

A qualitative comparison to other operational forecast models and a quantitative statistical model validation indicate that the RAMS predictions are capable of adding local scale, short-range (0–12-h) forecast value to the currently available regional-scale model forecasts. Results from several other simulations for this storm (Snook 1993) suggest that the forecast improvement by LAPS/RAMS is mostly due to the additional surface observations available to the LAPS analyses schemes and to the improved representation of topography that is allowed by using the 10-km horizontal grid spacing. The relative importance of the LAPS initialization and the improved topography is difficult to assess. Certainly, the improved topography representation plays a significant role in the forecast improvement when compared to coarser-resolution model predictions. Parallel simulations using the same 10-km topography with LAPS versus MAPS initializations (Snook 1993), however, clearly indicate significant improvement in the low-level LAPS initialized forecasts. This improvement is not evident in the middle and upper troposphere. Additional mesoscale detail

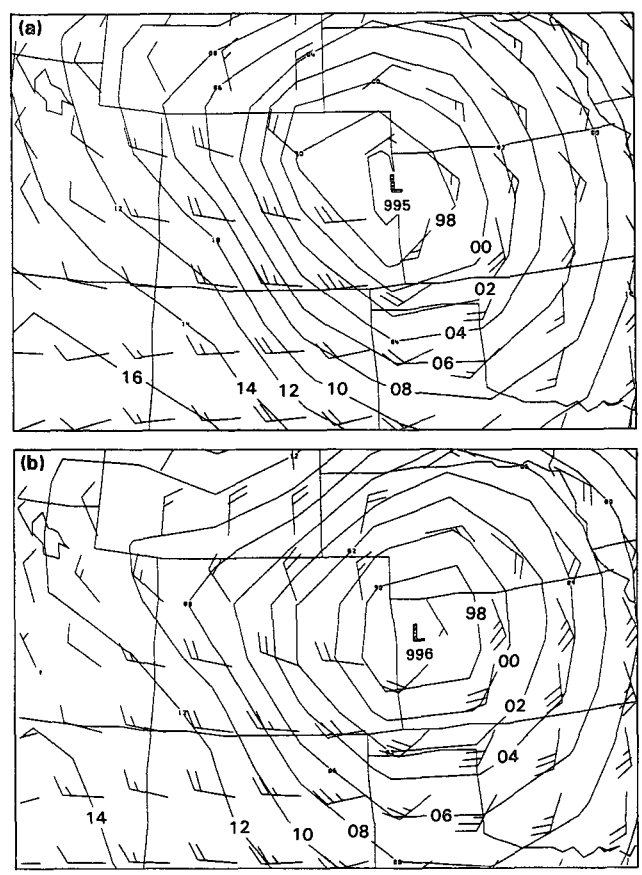

FIG. 17. NGM mean sea level pressure (mb) and surface wind (one full barb = 5 m s^{-1}) predictions from (a) the 6-h forecast valid at 1800 UTC 7 January and (b) the 12-h forecast valid at 0000 UTC 8 January 1992.

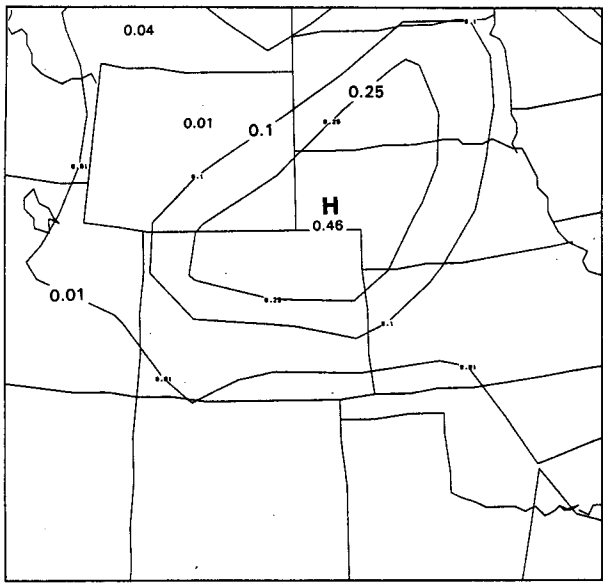

FIG. 18. NGM 12-h melted precipitation (in.) forecast valid at 0000 UTC 8 January 1992.

in the LAPS upper-air analyses suggests that LAPS initialized upper-air forecasts, especially very short-range predictions, should show improvement, but this is difficult to confirm due to the sparsity of upper-air observations.

A third objective of this paper is to demonstrate the ability to use the model output to provide an improved scientific understanding of mesoscale weather events. An evaluation of the model simulations in combination with previous investigations, actual observations, and other larger domain model simulations was useful in formulating a conceptual model of the case study system (Fig. 20). Three-dimensional views of the 7 January RAMS simulations provided insight into why the heavy snow fell east of the mountain barrier and east of the Longmont anticyclone convergence zone. A primary difference between this and other typical Front Range heavy snowstorms was the development of a mountain wave that created a region of dry downslope flow with little or no precipitation over the Front Range. The heavy snow band appears to be the result of two features: 1) a low-level area of ascent that developed within the eastern half of the mountain wave, and 2) moist, midlevel easterly component flow that ascended over the mountain wave. The two regions of ascent were coincident about 40 km east of the mountain barrier, and the model predicted a north–south band of heavy snow along this region. As the model-predicted easterly flow backed to northerly, the forecast snowfall decreased, which agreed with the surface observations of decreasing snowfall intensity.

The case study simulation was designed to emulate a real-time operational forecast using relatively inexpensive computer equipment that is currently available. The results show that a quasi-operational mesoscale numerical model can add significant value to currently available national domain operational model predictions and portend the ability to generate regional domain operational mesoscale numerical model predictions in the local weather forecast office.

The development of a real-time environment where RAMS is initialized with LAPS on a routine basis was established at FSL during late 1993 (Snook et al. 1995). Currently, the LSFC configuration (without explicit microphysics) is implemented. Every business day, RAMS is automatically initialized with 1200 UTC LAPS data and a 12-h forecast is generated. By using 0000 UTC initialized NGM forecasts as the lateral boundary nudging targets, the model is initiated at 1240 UTC and the 12-h forecast is completed within four hours. The explicit microphysics version (LMIC) requires nearly double the processing time, but quasi-operational implementation is expected shortly with the arrival of a next generation computer workstation at FSL. The objectives are twofold. First, real-time

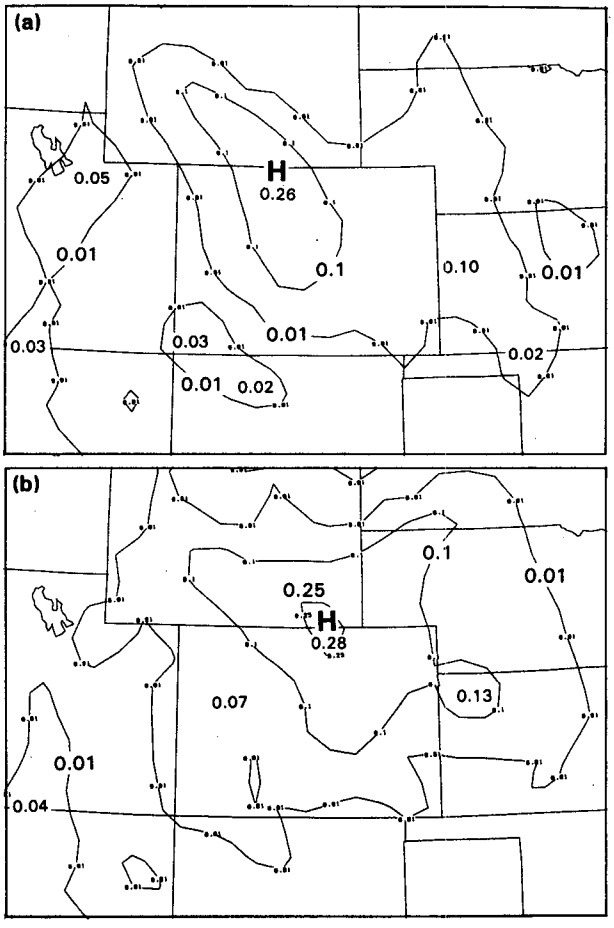

FIG. 19. MAPS 3-h melted precipitation (in.) forecasts from (a) the 3-h prediction valid at 1500 UTC and (b) the 6-h prediction valid at 1800 UTC 7 January 1992.

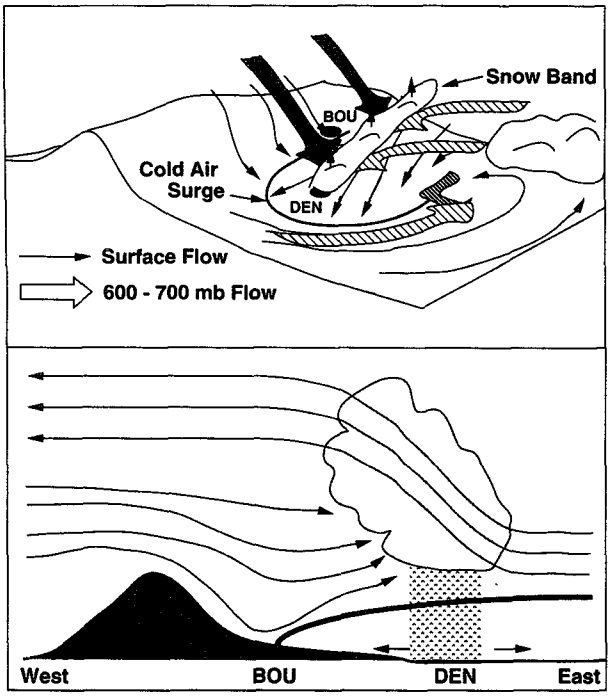

FIG. 20. Conceptual model of 7 January 1992 snow storm.

forecasts are available for critical objective review in a quasi-operational setting, such as the daily FSL weather briefing. Second, the daily model output would be available to complete a statistically significant quantitative evaluation. A statistical baseline for this operational LAPS/RAMS configuration is being established for comparison to other operational models and for evaluating possible improvements to the current LAPS/RAMS configuration.

An important component of the real-time LAPS/RAMS (Snook et al. 1995) is the use of three-dimensional (3D) visualization (e.g., AMS 1993). The high-resolution, full physics numerical model generates an enormous amount of output data. If the operational forecaster is to use the mesoscale model forecasts in a timely manner, one must have the capability to rapidly peruse the model predictions. Developing efficient 3D visualization techniques will be an important part of implementing an operational mesoscale prediction model. The case study investigation demonstrates the enormous potential of using the LAPS/RAMS real-time analysis and prediction system to forecast and display mesoscale systems in the local weather office.

Acknowledgments. The senior author acknowledges NOAA's Forecast Systems Laboratory sponsorship of research for his Ph.D. dissertation, from which this paper was derived. He also thanks his Ph.D. committee, Drs. Roger Pielke, John McGinley, David Randall, Richard Johnson, Paul Mielke, and William Cotton, as well as numerous others for their helpful suggestions and guidance. Dr. Jerome Schmidt was especially helpful with the case study analysis. Thanks to Larry Dunn and Steve Mullen for their thorough reviews of the manuscript. The authors are indebted to Dallas McDonald for her help with many of the publication details. Technical editing support was provided by Loys Balsley and Juanita Fullerton. Jim Adams provided figure drafting support. Additional support for this research was provided by funding from National Science Foundation Grant ATM-9017849.

APPENDIX

Quantitative Model Validation

Quantitative RAMS model validation is composed of analyzing several statistical measures generated from a comparison of observations and model predictions. Uncertainties arise, however, from the fact that the observations are not coincident with the model grid points. This requires either interpolating the model gridded data to the observation locations or analyzing the observations onto the model grid. The former process introduces uncertainties through the interpolation procedure and only provides results where observations exist. Likewise, uncertainties arise with the latter process, which also uses an interpolation procedure where the observations may not be representative of the model grid volume. Furthermore, the spatial availability of the observations dictates the scales resolvable within the analyzed field, which may be different from the resolvable scales of the model. Despite the uncertainties, the statistical evaluation used here will employ both forms of interpolation to present quantitative results using traditional and nontraditional schemes.

The quantitative comparison schemes are bias, root-mean-square (rms), and MRBP (Mielke 1991). Thompson (1993) describes the shortcomings of using verification methods (such as rms) that are based on a *squared* Euclidean distance function. Nonetheless, these schemes have been widely used and are in many cases the only statistics available for comparison to other model results. Mielke (1984, 1986) claims that to properly compare atmospheric models and observations, the comparison scheme should be based on an *ordinary* Euclidean distance function, since meteorological data exist in this space. The MRBP scheme described by Mielke (1991) adheres to this criteria and has been successfully applied by Tucker et al. (1989), Lee (1992), Thompson (1993), and Eastman (1993) for statistically analyzing numerical model output.

Bias and rms statistics are computed by subtracting the observation or analysis from the model forecast (RAMS–OBS). The MRBP statistic is determined for a particular meteorological variable by comparing a gridded analysis, derived from observations, with the model prediction that occupies the same grid. A chance corrected agreement measure, ρ, estimates the composite measurement agreement between the gridded

analysis and the model prediction. A ρ of 1.0 indicates perfect agreement between datasets while values of 0.0 or less indicate no agreement. Since the model predictions are nudged toward MAPS model forecasts at the lateral boundaries, the four outermost grid points on all sides are not included in the statistical computations. Hence, 2809 (53×53) grid points are considered.

Model validation is computed separately for surface observations and upper-air observations. At the surface, temperature, moisture, and wind observations are available from the 22-station FSL mesonet and from up to 51 surface aviation observation (SAO) locations. Model output is interpolated to the surface observation locations using an overlapping quadratics scheme. Since differences exist between the model and surface observation elevations, several adjustments are made to the interpolated model output. Model temperatures and wind speeds are adjusted by factors derived from a logarithmic wind profile (Louis 1979) using the lowest above-ground model level of 146 m for temperature and wind, a surface temperature observation level of 1.5 m, a surface wind observation level of 10 m, and the assigned model surface roughness value of 0.05 m. No adjustments are made to the model moisture variable. Bias and rms statistics are computed using every location where surface data are available. Spatial and temporal quality control of the observations is completed by the LAPS operational system.

Gridded analysis statistics at the surface are accomplished by comparing the LAPS surface analysis with predictions from the lowest model sigma level. Horizontal interpolation is not necessary because the LAPS and RAMS horizontal grids are coincident. However, some vertical extrapolation is implemented as discussed previously to account for the difference between the surface and lowest model sigma level elevations. In addition to the bias and rms statistics, the MRBP agreement measure (ρ) is calculated.

Model validation with upper-air observations is difficult because of the sparsity of data. The only available upper-air data sources within the model domain are the Denver rawinsonde and the Platteville, Colorado, wind profiler. A qualitative comparison of upper-air model predictions to the observations is accomplished by generating time series of upper-air model wind forecasts for direct comparison to the wind profiler data.

Upper-air gridded analysis statistics are accomplished by comparing the LAPS three-dimensional univariate analyses with the model predictions. Since LAPS (isobaric) and RAMS (sigma z) use different vertical coordinate systems, vertical interpolation is necessary on one of the datasets. First, LAPS analyses are interpolated to the RAMS sigma-z surfaces as discussed previously for model initialization. Bias, rms, and MRBP statistics are then computed on each sigma-z surface. Second, the rams predictions are interpolated back to the LAPS isobaric levels and the statistics are generated on more traditional isobaric surfaces.

a. Surface

Hourly bias and rms differences are computed for both RAMS simulations using all available surface observations compared to model predicted variables. Statistics are generated for temperature, dewpoint, wind speed, and wind direction. Note that about half of the observation locations are within the FSL mesonet area (Fig. 1). Hence, when evaluating the statistics, the results will be weighted toward the model performance in this region. Statistical results are very close for both simulations, except for dewpoint where the LMIC simulation shows an average dewpoint of about 1° warmer than the LSFC average dewpoint.

Figures A1 and A2 depict the LMIC results. The temperature bias remains less than 0.5 K except after 11 h. Rms temperature results are generally around 2 K through the forecast period. A 1 to 2 K moist dewpoint bias is noted for the LMIC simulation. Although the LSFC dewpoint bias is closer to zero, the LMIC

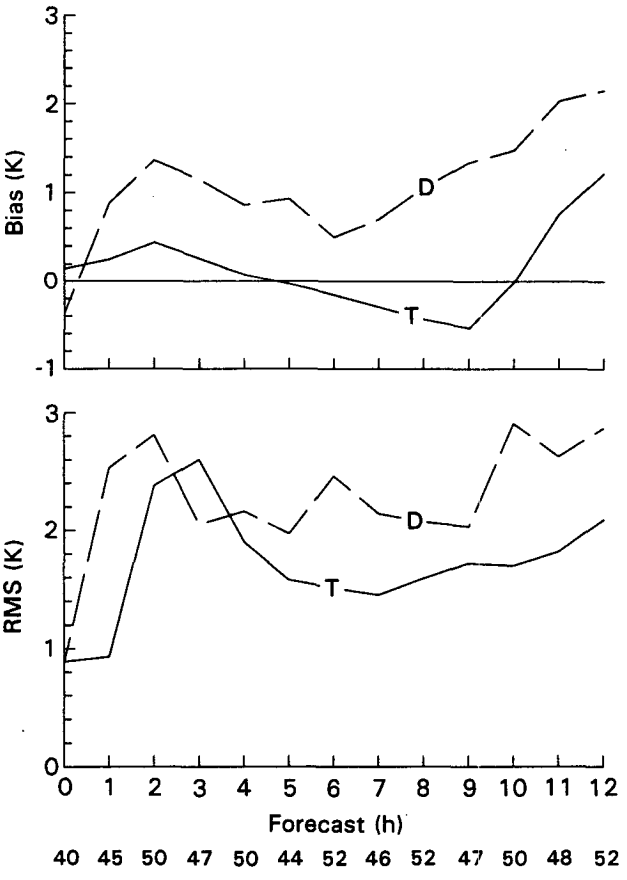

FIG. A1. Hourly bias and rms differences of temperature (K) and dewpoint (K) for the RAMS (LMIC) simulation compared to surface observations. Differences are computed by subtracting the observations from RAMS. The solid line (T) represents temperature and the dashed line (D) represents dewpoint. Numbers under the forecast time indicate the number of observations available to the comparison computations.

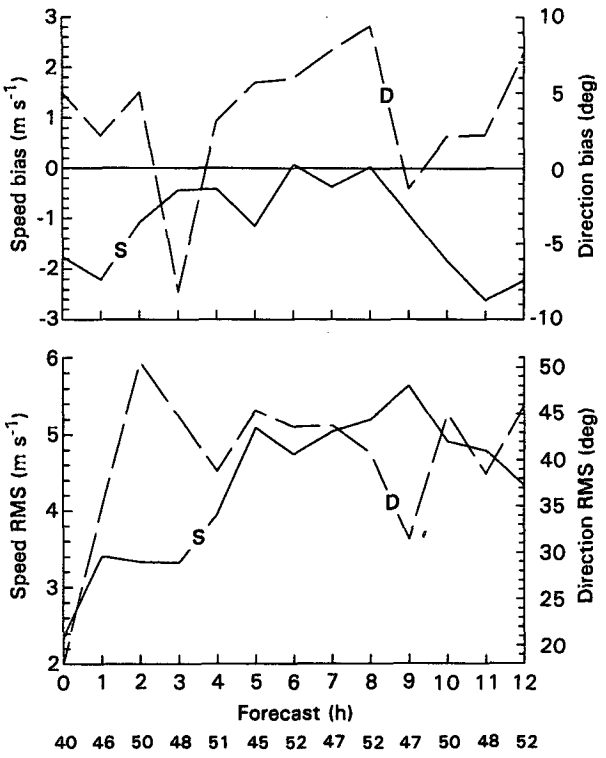

FIG. A2. As in Fig. A1 except for wind speed (m s^{-1}, solid line) and wind direction (degrees, dashed line).

rms differences of 2–3 K slightly outperformed the LSFC simulation.

Wind speed forecasts are quite good with a slight underforecast of 1–2 m s^{-1}. Rms differences range from about 3 m s^{-1} during the early forecast period to around 5 m s^{-1} after 5 h. A positive wind direction bias of 5–10 degrees is observed during most of the forecast period. Since the lowest model level is higher than the actual surface observation elevation, the model level winds experience less surface friction effects than the surface level winds. Hence, a positive bias in wind direction can be expected when comparing winds from these two levels. A correction to the model-predicted wind direction is not applied to compensate for this effect. Wind direction rms differences generally range from 35 to 45 degrees.

Hourly bias, rms, and MRBP statistics are calculated for both simulations using LAPS gridded surface analyses compared to RAMS predictions of temperature, mixing ratio, wind speed, and wind direction. The advantage of the gridded analysis comparison is that the statistical results are representative of the whole domain. However, the method assumes that the LAPS gridded analyses represent the actual surface conditions, which may not be a good assumption in data-sparse areas. The LAPS system incorporates all available local data sources with conventional data sources in an attempt to resolve mesoscale (down to 40 km) features using a 10-km horizontal grid interval. However, even with the additional local data sources, the resolution of the observations is not nearly sufficient to fully support the 40-km grid resolution over the whole domain used by LAPS and RAMS. Hence, the model-predicted fields will contain higher-resolution information than the LAPS gridded analyses resulting in an unfair statistical comparison (Thompson 1993). If the model predicts a mesoscale feature that is not resolvable by the analysis, it may appear that the model performed poorly, when in fact the model may have correctly predicted the feature. In other words, the model is penalized for generating any features with resolution greater than the observations, regardless of the accuracy.

MRBP statistics from the LMIC simulation are presented in Fig. A3. The MRBP agreement measures are very good for temperature, with values around 90%, and moisture, with values in the 80%–90% range. Wind speed and direction agreement measures are significantly lower.

b. *Upper air*

Upper-air model validation statistics are computed by comparing the model forecast with the corresponding LAPS three-dimensional analysis on each model sigma level. Since upper-air observations are even more sparse than surface observations, the possibility of the model forecasts containing higher-resolution information than the LAPS gridded analyses is even greater.

MRBP agreement measure statistics of temperature, perturbation Exner function (π^*), relative humidity, u, v, and total wind speeds, and absolute vorticity are illustrated in Fig. A4 for the 6- and 12-h LMIC forecasts. The mass variables (temperature and π^*) performed best, followed by wind, and then moisture,

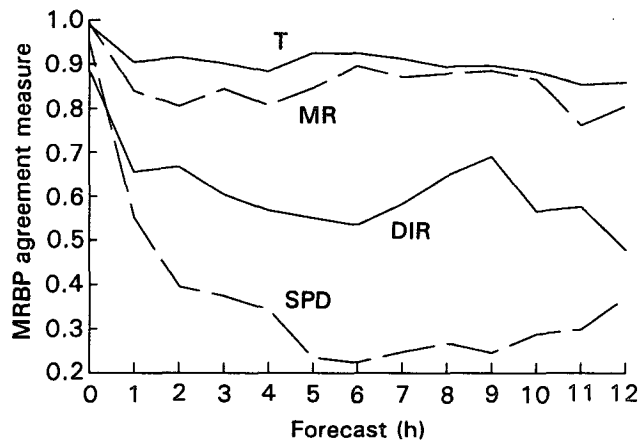

FIG. A3. MRBP agreement measure for the RAMS (LMIC) simulation compared to the LAPS gridded surface analyses. Lines represent agreement measures of temperature (T), mixing ratio (MR), wind direction (DIR), and wind speed (SPD), respectively.

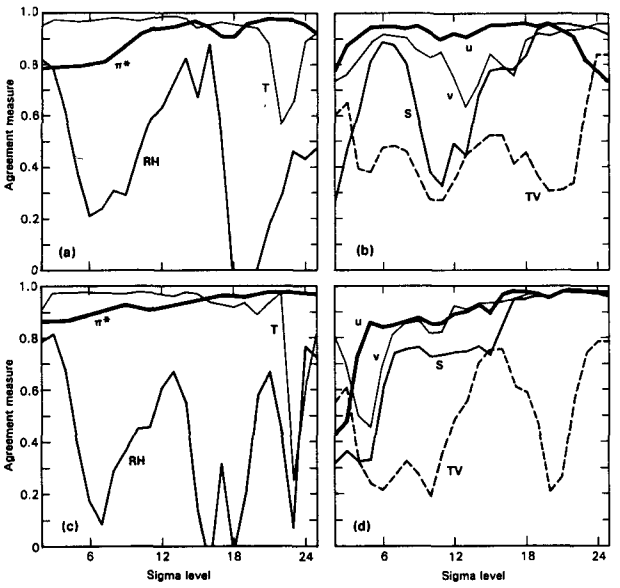

FIG. A4. Upper-air MRBP statistics for the RAMS (LMIC) simulation compared to LAPS gridded upper-air analyses. Agreement measure is presented from the 6-h forecast valid at 1800 UTC 7 January 1992 for (a) perturbation Exner function (π^*), temperature (T), relative humidity (RH), and (b) u-component wind (u), v-component wind (v), wind speed (S), total vorticity (TV), and from the 12-h forecast valid at 0000 UTC 8 January for (c) thermodynamic and (d) wind variables.

similar to results found by Thompson (1993) using RAMS initialized with MAPS data. Since moisture typically exhibits the greatest amount of upper-level atmospheric spatial variability, the problem of insufficient observations affects this comparison the most. Six-hour temperature and perturbation Exner function agreement measures are mostly greater than 90%. Relative humidity statistics indicate good agreement (~80%) near the surface, less agreement around sigma levels 6–8 (~600 mb), increased agreement up to the tropopause, and no agreement in the vicinity of the tropopause (sigma levels 18–20). Here U- and v-component wind speeds show mostly greater than 80% agreement except around sigma level 13 (~400 mb), where the v-component shows less agreement. Total wind speed agreement reflects the combined performance of u and v. The 12-h agreement measures are similar, except for a drop in relative humidity agreement and less agreement with the wind variables in the lower levels.

Thompson (1993) computed similar MRBP statistics for an entire winter season of RAMS forecasts initialized with data derived from the 60-km grid increment MAPS analyses. Thompson used a two-nested grid configuration with a 25-km grid increment inner mesh covering most of Colorado. MRBP agreement measures were computed by comparing the 25-km grid interval RAMS predictions with 100-km grid increment analyses, which, as Thompson noted, is an unfair statistical comparison as discussed above. A comparison of results for this one case (7 January 1992) to Thompson's whole season results indicates significant improvement in all variables except upper-level moisture. Of particular interest is the significant improvement near the surface in mass (from 50% to 90%), moisture (from 30% to 80%), and wind speed (from 25% to 55%). Thompson noted that numerical models typically show poor agreement at the surface for temperature and relative humidity. The results from the 7 January 1992 case study suggest that the additional mesoscale surface observations have improved the predictions of surface temperature and moisture, and the surface analyses used for comparison, resulting in much better statistical agreement. While the surface forecast improvements are encouraging, a much larger comparison sample is necessary to provide statistically significant results valid for an entire winter season.

REFERENCES

Abbs, D. J., and R. A. Pielke, 1987: Numerical simulations of orographic effects on NE Colorado snowstorms. *Meteor. Atmos. Phys.*, **37**, 1–10.

Albers, S. C., 1989: A severe weather forecast scheme incorporating mesoscale analyses. Preprints, *12th Conf. on Weather Analysis and Forecasting*, Monterey, CA, Amer. Meteor. Soc., 242–246.

AMS, 1993: Cover figure. Program, *73rd Annual Meeting of the American Meteorological Society*, Anaheim, CA, Amer. Meteor. Soc.

Benjamin, S. G., K. A. Brewster, R. Brümmer, B. F. Jewett, T. W. Schlatter, T. L. Smith, and P. A. Stamus, 1991: An isentropic three-hourly data assimilation system using ACARS aircraft data. *Mon. Wea. Rev.*, **119**, 888–906.

Birkenheuer, D., 1991: An algorithm for operational water vapor analyses integrating GOES and dual-channel microwave radiometer data on the local scale. *J. Appl. Meteor.*, **30**, 834–843.

Chen, C., and W. R. Cotton, 1983: A one-dimensional simulation of the stratocumulus-capped mixed layer. *Bound.-Layer Meteor.*, **25**, 289–321.

Cotton, W. R., G. Thompson, and P. W. Mielke Jr., 1994: Realtime mesoscale prediction on workstations. *Bull. Amer. Meteor. Soc.*, **75**, 349–362.

Cram, J. M., 1990: Numerical simulation and analysis of the propagation of a prefrontal squall line. Ph.D. thesis, Colorado State University, Fort Collins, CO, 332 pp.

Davies, H. C., 1976: A lateral boundary formulation for multi-level prediction models. *Quart. J. Roy. Meteor. Soc.*, **102**, 405–418.

Dudhia, J., 1993: A nonhydrostatic version of the Penn State–NCAR mesoscale model: Validation tests and simulation of an Atlantic cyclone and cold front. *Mon. Wea. Rev.*, **121**, 1493–1513.

Dunn, L. B., 1987: Cold-air damming by the Front Range of the Colorado Rockies and its relationship to locally heavy snows. *Wea. Forecasting*, **2**, 177–189.

——, 1988: Vertical motion evaluation of a Colorado snowstorm from a synoptician's perspective. *Wea. Forecasting*, **3**, 261–272.

——, 1992: Evidence of ascent in a sloped barrier jet and an associated heavy-snow band. *Mon. Wea. Rev.*, **120**, 914–924.

Eastman, J. L., 1993: A numerical study and tracer evaluation of transport and diffusion in a lake breeze. M.S. thesis, Colorado State University, Fort Collins, CO, 112 pp.

Fawcett, E. B., and H. K. Saylor, 1965: A study of the distribution of weather accompanying Colorado cyclogenesis. *Mon. Wea. Rev.*, **93**, 359–367.

Flatau, P. J., G. J. Tripoli, J. Verlinde, and W. R. Cotton, 1989: The CSU-RAMS cloud microphysical module: General theory and

code documentation. Dept. of Atmospheric Science Paper No. 451, Colorado State University, Fort Collins, CO, 88 pp.

Howard, K. W., and E. I. Tollerud, 1988: The structure and evolution of heavy-snow-producing Colorado cyclones. Preprints, *Palmen Symp. on Extratropical Cyclones and Their Role in the General Circulation,* Helsinki, Finland, 168–171.

Junker, N. W., J. E. Hoke, and R. H. Grumm, 1989: Performance of NMC's regional models. *Wea. Forecasting,* **4,** 368–390.

Lee, T. J., 1992: The impact of vegetation on the atmospheric boundary layer and convective storms. Ph.D. thesis, Colorado State University, Fort Collins, CO, 137 pp.

Lilly, D. K., 1981: Doppler radar observations of upslope snowstorms. Preprints, *Second Conf. on Mountain Meteorology,* Steamboat Springs, CO, Amer. Meteor. Soc., 346–353.

Louis, J. F., 1979: A parametric model of vertical eddy fluxes in the atmosphere. *Bound.-Layer Meteor.,* **17,** 187–202.

Marwitz, J. D., and J. Toth, 1993: A case study of heavy snowfall in Oklahoma. *Mon. Wea. Rev.,* **121,** 648–660.

McGinley, J. A., 1989: The local analysis and prediction system. Preprints, *12th Conf. on Weather Analysis and Forecasting,* Monterey, CA, Amer. Meteor. Soc., 15–20.

——, 1995: Opportunities for high resolution data analysis, prediction, and product dissemination within the local weather office. Preprints, *14th Conf. on Weather Analysis and Forecasting,* Dallas, TX, Amer. Meteor. Soc., in press.

——, S. C. Albers, and P. A. Stamus, 1991: Validation of a composite convective index as defined by a real-time local analysis system. *Wea. Forecasting,* **6,** 337–356.

Mielke, P. W., 1984: Meteorological applications of permutation techniques based on distance functions. *Handbook of Statistics,* Vol. 4, P. R. Krishnaiah and P. K. Sen, Eds., North-Holland, 813–830.

——, 1986: Non-metric statistical analysis: Some metric alternatives. *J. Stat. Plan. Inference,* **13,** 377–387.

——, 1991: The application of multivariate permutation methods based on distance functions in the earth sciences. *Earth-Sci. Rev.,* **31,** 55–71.

NOAA, 1992: Storm data and unusual weather phenomena, January 1992. National Climatic Data Center, 34, 60 pp.

Papineau, J. M., 1992: A performance evaluation of the NGM and RAMS models for the 29–30 March 1991 Front Range storm. M.S. thesis, Colorado State University, Fort Collins, CO, 73 pp.

Pielke, R. A., W. R. Cotton, R. L. Walko, C. J. Tremback, W. A. Lyons, L. D. Grasso, M. E. Nicholls, M. D. Moran, D. A. Wesley, T. J. Lee, and J. H. Copeland, 1992: A comprehensive meteorological modeling system—RAMS. *Meteor. Atmos. Phys.,* **49,** 69–91.

Rasmussen, R., M. Politovich, J. Marwitz, W. Sand, J. McGinley, J. Smart, R. Pielke, S. Rutledge, D. Wesley, G. Stossmeister, B. Bernstein, K. Elmore, N. Powell, E. Westwater, B. B. Stankov, and D. Burrows, 1992: Winter Icing and Storms Project (WISP). *Bull. Amer. Meteor. Soc.,* **73,** 951–974.

Reinking, R. F., and J. F. Boatman, 1986: Upslope precipitation events. *Mesoscale Meteorology and Forecasting,* P. S. Ray, Ed., Amer. Meteor. Soc., 437–471.

Ross, B. B., 1986: An overview of numerical weather prediction. *Mesoscale Meteorology and Forecasting,* P. S. Ray, Ed., Amer. Meteor. Soc., 720–751.

Schlatter, T. W., D. V. Baker, and J. F. Henz, 1983: Profiling Colorado's Christmas Eve blizzard. *Weatherwise,* **36,** 60–66.

Schmidt, J. M., and J. S. Snook, 1992: A numerical and observational investigation of the 7 January 1992 Denver, Colorado, blizzard: A regional-scale perspective. Preprints, *Sixth Conf. on Mountain Meteorology,* Portland, OR, Amer. Meteor. Soc., 161–165.

Scorer, R. S., 1949: Theory of waves in the lee of mountains. *Quart. J. Roy. Meteor. Soc.,* **75,** 41–56.

Smagorinsky, J., 1963: General circulation experiments with the primitive equations. Part I: The basic experiment. *Mon. Wea. Rev.,* **91,** 99–164.

Smith, R. B., 1979: The influence of mountains on the atmosphere. *Advances in Geophysics,* Vol. 21, Academic Press, 87–230.

Smith, T. L., and S. G. Benjamin, 1993: Impact of network wind profiler data on a 3-h data assimilation system. *Bull. Amer. Meteor. Soc.,* **74,** 801–807.

Snook, J. S., 1992: Current techniques for real-time evaluation of conditional symmetric instability. *Wea. Forecasting,* **7,** 430–439.

——, 1993: An investigation of Colorado Front Range winter storms using a nonhydrostatic mesoscale numerical model designed for operational use. Ph.D. thesis, Colorado State University, Fort Collins, CO, 373 pp.

——, and J. M. Schmidt, 1992: A numerical and observational investigation of the 7 January 1992 Denver, Colorado, blizzard: Local-scale perspective. Preprints, *Sixth Conf. on Mountain Meteorology,* Portland, OR, Amer. Meteor. Soc., 101–105.

——, J. M. Cram, and J. M. Schmidt, 1995: LAPS/RAMS: A nonhydrostatic mesoscale numerical modeling system configured for operational use. *Tellus,* in press.

Thompson, G., 1993: Prototype real-time mesoscale prediction during the 1991–1992 winter season and statistical verification of model data. M.S. thesis, Colorado State University, Fort Collins, CO, 105 pp.

Tollerud, E. I., K. W. Howard, and X.-P. Zhong, 1991: Jet streaks and their relationship to heavy precipitation in Colorado Front Range winter storms. Preprints, *First Int. Symp. on Winter Storms,* New Orleans, LA, Amer. Meteor. Soc., 97–100.

Tremback, C. J., 1990: Numerical simulation of a mesoscale convective complex: Model development and numerical results. Ph.D. thesis, Colorado State University, Fort Collins, CO, 247 pp.

——, and R. Kessler, 1985: A surface temperature and moisture parameterization for use in mesoscale numerical models. *Seventh Conf. on Numerical Weather Prediction,* Montreal, Canada, Amer. Meteor. Soc., 355–358.

Tucker, D. F., P. W. Mielke, and E. R. Reiter, 1989: The verification of numerical models with multivariate randomized block permutation procedures. *Meteor. Atmos. Phys.,* **40,** 181–188.

Warner, T. L., and N. L. Seaman, 1990: A real-time, mesoscale numerical weather-prediction system used for research, teaching, and public service at The Pennsylvania State University. *Bull. Amer. Meteor. Soc.,* **71,** 792–805.

Wesley, D. A., 1991: An investigation of the effects of topography on Colorado Front Range winter storms. Ph.D. thesis, Colorado State University, Fort Collins, CO, 197 pp.

——, and R. A. Pielke, 1990: Observations of blocking-induced convergence zones and effects on precipitation in complex terrain. *Atmos. Res.,* **25,** 235–276.

——, J. F. Weaver, and R. A. Pielke, 1990: Heavy snowfall during an arctic outbreak along the Colorado Front Range. *Nat. Wea. Digest,* **15,** 2–19.

Young, G. S., and R. H. Johnson, 1984: Meso- and microscale features of a Colorado cold front. *J. Climate Appl. Meteor.,* **23,** 1315–1325.